Sol-Gel Derived Silicate-based Titanium-containing Bioactive Glass for Enamel Remineralization

Sophia Smith
Department of Mining and Materials Engineering
McGill University, Montreal, QC, Canada
November 2019

A thesis submitted to McGill University in partial fulfillment of the requirements for the degree of Master of Engineering (Thesis)

For my family

Abstract

Enamel is the hardest and most heavily mineralized material in the human body. It is 96% mineral (hydroxyapatite), 4% organic matter and a variety of trace metallic elements. The enamel layer is naturally susceptible to demineralization and, as it is not a living tissue, is unable to fully remineralize by biological methods. Demineralization causes issues in overall tooth health, ranging in severity from dental sensitivity to cavity formation. When placed in physiological fluid, bioactive glasses undergo a transformation from glass to hydroxyapatite, making bioactive glass a promising material to induce enamel remineralization. In fact, certain bioactive glasses are commercially available in over the counter toothpastes. However, these bioactive glasses simply replace the lost hydroxyapatite, without adding new properties to the remineralized layer. Doping the bioactive glass with metallic ions can impart desirable and unique properties that are not inherent to natural hydroxyapatite.

Titanium exists in trace amounts in native enamel and its presence has been correlated with increased tooth hardness and brightness. Synthetic titanium substituted hydroxyapatite exhibits better mechanical, antibacterial and aesthetic properties than unmodified hydroxyapatite. Due to these improved properties, and a significantly increased bone-forming cellular response, titanium-substituted hydroxyapatite has applications extending beyond dentistry and into the broader bone tissue engineering field.

In this thesis, we use the sol-gel method to synthesize a titanium-containing silicate-based bioactive glass aimed at generating titanium substituted hydroxyapatite. Titanium is homogenously distributed throughout our glass, without modifying the structure or amorphous nature. After 14 days immersion in simulated body fluid, the glass forms a titanium substituted hydroxyapatite. We show that the titanium-containing glass is non-toxic to cells. Furthermore, cells in contact with titanium-containing bioactive glass exhibit significantly higher levels of differentiation towards bone-formation. From synthesis, to characterization of the mineralized layer, to cellular response our results demonstrate that this titanium-containing bioactive glass has potential both for enamel remineralization and application in the broader field of bone tissue engineering.

Résumé

L'émail est le matériau le plus dur et le plus fortement minéralisé du corps humain. Il contient 96% de minéraux (hydroxyapatite), 4% de matière organique, et une variété d'éléments traces métalliques. La couche d'émail est naturellement prédisposée à la déminéralisation et, comme il ne s'agit pas d'un tissu vivant, elle ne peut pas être complètement reminéralisée par des méthodes biologiques. La déminéralisation pose des problèmes pour la santé générale des dents, allant de leur sensibilité à la formation de cavités. Lorsqu'ils sont placés dans un liquide physiologique, les verres bioactifs subissent une transformation de verre en hydroxyapatite, faisant du verre bioactif un matériau prometteur pour induire la reminéralisation de l'émail. En effet, certains verres bioactifs sont disponibles dans le commerce dans les dentifrices en vente libre. Cependant, ces verres bioactifs remplacent simplement l'hydroxyapatite perdue, sans ajouter de nouvelles propriétés à la couche reminéralisée. Le dopage du verre bioactif avec des ions métalliques peut conférer des propriétés uniques et souhaitables qui ne sont pas inhérentes à l'hydroxyapatite naturelle.

Le titane existe à l'état de traces dans l'émail natif, et sa présence a été corrélée avec l'augmentation de la dureté et de la brillance des dents. L'hydroxyapatite substituée par du titane synthétique présente de meilleures propriétés mécaniques, antibactériennes, et esthétiques que l'hydroxyapatite non modifiée. En raison de ces propriétés améliorées et d'une réponse cellulaire considérablement accrue formant l'os, l'hydroxyapatite substituée par du titane a des applications qui vont au-delà de la dentisterie et dans le domaine plus général de l'ingénierie du tissu osseux.

Dans cette thèse, nous utilisons la méthode sol-gel pour synthétiser un verre bioactif à base de silicate contenant du titane dans le but de générer de l'hydroxyapatite à substitution titane. Le titane est distribué de manière homogène dans tout le verre, sans modifier sa structure ni sa nature amorphe. Après 14 jours d'immersion dans un fluide corporel simulé, le verre forme de l’hydroxyapatite substituée par du titane. Nous montrons que le verre contenant du titane est non toxique pour les cellules. De plus, les cellules en contact avec du verre bioactif contenant du titane présentent des niveaux de différenciation significativement plus élevés vers la formation d'os. De la synthèse, à la réponse cellulaire, en passant par la caractérisation de la couche

minérale, nos résultats démontrent que ce verre bioactif contenant du titane présente un potentiel à la fois pour la reminéralisation de l'émail et pour une application dans le domaine plus vaste de l'ingénierie tissulaire osseuse.

Acknowledgements

First and foremost, I would like to express my deepest gratitude for the continued advice and guidance of Professor Marta Cerruti. I am so thankful to have been able to be a part of your group and to be given the flexibility to explore a topic that holds such interest to me. Thank you for your generosity with your time and ideas throughout my time as a Master's student.

My thanks also go to Dr. Simon Tran for his time and guidance in welcoming me to his lab space to carry out cell experiments. In particular, I would like to thank Osama ElKashty for his generosity with his time throughout the course of those experiments. Without his help, this would have been a much more difficult experience. Finally, I would like to thank Yara Oweis for her kindness, assistance with running XPS and guidance throughout my time in this program.

I would also like to acknowledge everyone who helped with experimental training, safety training, characterization work and administrative matters: Dr. Lihong Shang, Ranjan Roy, Aleksandra Djuric, Dr. Florence Paray, Dr. Ashlee Howarth, Barbara Hanley, June Persaud and Leslie Bernier. Additionally, thanks go to the members of the Biointerface Lab group who aided me in running experiments: Emily Buck, Dhanalakshmi Jeyachandran, and Kirklann Lau.

Thank you to all members of the Biointerface Lab, for making my time enjoyable, especially to Danae Guerra, Emily Buck, Yiwen Chen and Ophélie Gourgas, who so kindly took me under their wings and were excellent friends. I would also like to express my gratitude to Dr. William Lepry for acting as my mentor for several years now. He introduced me to bioactive glass in my undergraduate research and has continued to be a guiding force since. A special thanks also goes to my office mates, Kirk Lau, Tiffany Turner, Ahmad Saad, Aniruddha Das and Hao Li for making me laugh every day and listening to me when I needed to chat.

Finally, thanks go to my family and friends who have supported me through two degrees at McGill. Thank you to Madeline Perrin, Joel Grant, Hunter Kimmitt, Kate Knowles, Lina Du and Laurence Perron for being there for me every step of the way. I would also like to acknowledge

Richard Church, for his love and support. I would like to thank my parents for their emotional and financial support throughout my entire education. To my mother, Tracey, thank you so much for providing me with the tools to be able to complete this portion of my life. To my siblings, Babette and Lilith, your kindness and love has been a rock to me throughout this journey. You helped me in my worst moments and celebrated with me in my best. I look forward to continuing this in the next stage of my life.

Table of Contents

Table of Figures

Table of Tables

Thesis Structure

This thesis was compiled in compliance with the formatting and content required by the Graduate and Postdoctoral Studies at McGill University. Chapter 1 provides a general background, motivations and objectives for the project. Chapter 2 provides a detailed literature covering enamel, demineralization, current remineralization technologies, bioactive glass and the introduction of metallic ions to glass for tunable applications. Chapters 3 and 4 show results of the objectives outlined in Chapter 1. Chapter 5 provides a summary of the completed work and gives a scope for future work.

Contributions of the Authors

The work that comprises this thesis was written by the candidate under the supervision of Professor Marta Cerruti and is presented in Chapters 3 and 4. The candidate proposed, designed, and conducted the majority of the experiments and analyzed the resulting data. Critical research advice and guidance was provided by Prof. Marta Cerruti, in addition to a thorough review of all submitted material. Data presented in Chapter 3 was acquired with the assistance of Dr. Ashlee Howarth (surface area analysis), Yara Oweis (XPS), Dhanalakshmi Jeyachandran (SEM), and Kirklann Lau (SEM and EDS). Dr Simon Tran and Osama ElKashty provided essential guidance on experimental setup for the results outlined in Chapter 4. Osama ElKashty also worked alongside the candidate to collect the data shown in Chapter 4.

Chapter 1: General Overview

1.1 Introduction

Enamel is the hardest and most heavily mineralized material in the human body [1]. It is composed of 96% mineral (hydroxyapatite), 4% organic matter and a variety of trace metallic elements such as selenium, chromium and titanium [2]. Titanium (Ti) presence has been correlated with increased tooth hardness and brightness, both sought after attributes for clinical applications [2, 3]. The enamel layer is susceptible to demineralization and is unable to fully remineralize by biological methods as it is not living tissue. As the tooth demineralizes, issues arise in overall tooth health, ranging in severity from dental sensitivity to the formation of cavities [4]. There are several methods to remineralize enamel, one of which is bioactive glass. This material is reactive when placed in physiological fluid, undergoing a transformation from glass to hydroxyapatite, the main mineral component of enamel [5].

Bioactive glass, first invented in 1969 by Dr Larry Hench, has since emerged as a leader in the field of tissue engineering [6]. Applications range from the repair of defects in hard tissue to enamel remineralization with great commercial success [7]. The formation of a hydroxyapatite (HA) layer and the ability to release ions results in osteo-conductive and osteo-stimulative properties that sets bioactive glass apart [8]. Synthesis is achieved by a melt-quenched process or a sol-gel process. Sol gel processing allows for glass with more variable composition and higher surface area than melt derived processing routes [9].

Bioactive glass networks also support the possibility of ionic doping [10]. Numerous metallic oxides have been incorporated as network modifiers, resulting in modifications to the physical and chemical properties of the glass. The majority of the metals incorporated are released to the local physiological environment, generally as targeted antibacterial applications [10]. The release rate of ions is controlled by glass dissolution rate in conjunction with the rate of tissue healing [10, 11].

Previous research has explored the creation of synthetic HA with metallic ion substitutions [12]. Synthetic Ti substituted HA exhibits better mechanical, antibacterial and aesthetic properties than unmodified HA [13-15]. Furthermore, Ti-substituted HA has exhibited improved cell response both in terms of cell attachment/viability and osteogenic differentiation [14, 16]. This would allow for applications of a bioactive glass with Ti inclusion to extend beyond dentistry and enamel remineralization, into the broader bone tissue engineering field.

1.2 Aim, Hypothesis and Objectives

The aim of this research was to create a sol-gel derived Ti-containing bioactive glass, and in so doing generate a Ti containing HA surface layer upon contact with physiological fluid. We hypothesized that by altering the glass composition, Ti could be retained within the glass network and ultimately within the eventual HA layer. The retention of Ti would make this material an excellent candidate for enamel remineralization, simultaneously regenerating HA that is lost over the course of life and delivering Ti ions to the enamel surface, in order to improve mechanical and aesthetic properties.

Furthermore, we hypothesised that this material could have applications beyond dentistry into the broader field of bone tissue engineering. We made this claim since synthetic HA with Ti inclusion induces a more favourable osteogenic response than non-Ti HA.

We formulated the following research goals:

1. Fabrication of a Ti-containing sol-gel bioactive glass
2. See how the inclusion of Ti induces differences in surface area, reactivity and bioactivity
3. Investigate the effect of Ti inclusion in bioactive glass on cell viability and osteogenic differentiation

Chapter 2: Literature Review

2.1 Enamel

2.1.1 Overview

Enamel is the hardest and most heavily mineralized material in the human body. It is the part of the tooth that is most visible (Figure 2.1). It is composed of 96% mineral and 4% organic matter [1]. The structure is highly organized, with densely packed hydroxyapatite (HA) crystals growing in formations called enamel rods. The study and understanding of enamel are integral to the dental profession as much of the day-to-day clinical practice revolves around enamel demineralization prevention and techniques to promote remineralization.

Figure 2.1: Typical Human Tooth [1]

During demineralization, minerals, primarily calcium (Ca), are removed from the tooth surface. Since the tooth is not comprised of living tissue it cannot remineralize by biological methods [1]. As the tooth demineralizes, issues arise in overall tooth health, ranging in severity from dental sensitivity to the formation of cavities [1]. According to the Canadian Dental Association, Canadians have some of the best access to dental care worldwide. However, there are still significant issues with dental health and demineralization. In 2017, 38% of 12 year old children in Canada had one or more permanent teeth affected by cavities [17]. Enamel is also centerpiece of the smile, one of the most recognisably human attributes. The health and aesthetic

appearance of the smile has great impact on self-confidence and interpersonal relationships. Additionally, poor oral health has a great economic impact on society.

The issues relating to demineralization are far reaching. Therefore, people are very interested in developing remineralization techniques, to replace lost minerals and repair lost structural integrity. These techniques range from toothpastes to mouthwashes and include materials such as fluoride, Ca and bioactive glass.

2.2 Enamel Structure

2.2.1 Hydroxyapatite

Enamel is highly mineralized with 95-97wt% attributed to HA [4]. HA ($Ca_{10}(PO_4)_6(OH_2)$) is a calcium phosphate (Ca:P ratio is 1.67) [18]. Beyond enamel, a form of HA is roughly 70 wt% of all human bone. A commonly synthetically manufactured biomaterial, it is favoured for its ability to support bone growth [18].

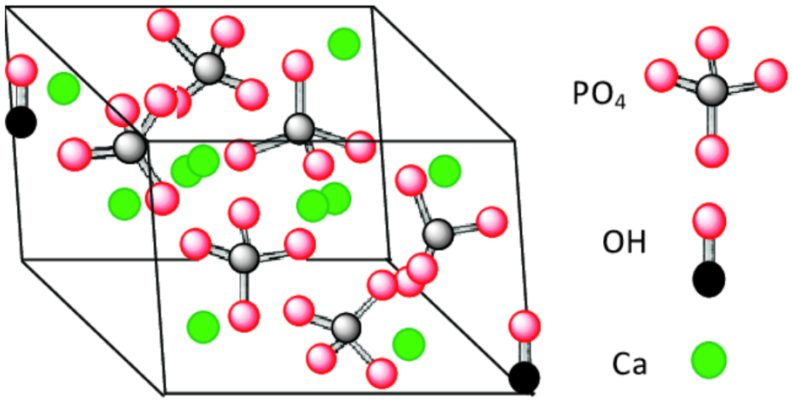

Figure 2.2: Structure of hydroxyapatite crystals [19]

HA crystals (Figure 2.2) have a loosely packed hexagonal structure. The unit cell comprises of 10 cation sites (Ca), arranged in two non-equivalent positions. Six of these sites are at the apexes of equilateral triangles, and each Ca is surrounded by seven oxygen atoms. The other four Ca sites are along the column and are each surrounded by nine oxygens [18]. P within the material interacts with the oxygen to form PO_4 tetrahedra. These tetrahedra do not share oxygens and are held together by Ca atoms. The hydroxyl groups within HA are important to the structure. They are located either above or below the symmetry position in the c-direction. The deviation

of hydroxyl groups from the symmetry position gives rise to four possible locations within the unit cell, on either side of the two symmetry positions [20].

The apatite structure of HA allows for a wide variety of both anionic and cationic substitutions within the lattice. This substitution is an effective way to modify the properties of HA to fit a targeted application. As substitution into HA usually involves the substitution of Ca, the relative size of the substituting ion will either cause the lattice to expand or contract. Inclusion of ions with an ionic radius smaller than that of Ca would result in smaller unit cell than unmodified HA [21]. The HA structure shrinks in volume as a result of shrinkage of the crystal lattice volume [21].

2.2.2 Chemical Composition and Structure

The distribution of the mineral and organic phase within enamel is not uniform. Enamel typically grows in basic units of structure, referred to as enamel rods or prisms. Each rod is composed of about 1000 elongated HA crystals, with the long axis of the rod running perpendicular to the underlying dentin, along the dentino-enamel junction [22]. Enamel rods have a diameter ranging from 3 to 7 μm. The rods interlock closely with each other, with organic material most commonly occurring in the outer regions of the rods and in the inter-rod regions and functioning as a glue for the apatite crystals [22]. The cross-sectional profile varies from circular to the more common keyhole shape. Figure 2.3 shows the overall keyhole shape shaded in grey.

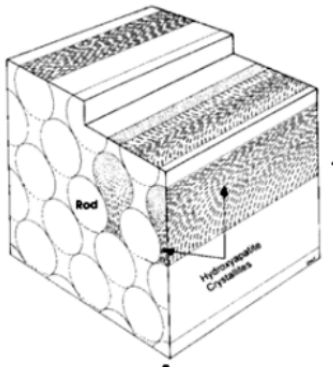

Figure 2.3: Schematic of enamel rod and inter-rod structure [5]

The keyhole shape is divided into a head and tail portion. The more rounded, larger end of the keyhole makes the head, and is well defined by a proteinaceous rod sheath (about 0.5μm thick). The tail region is less well defined and becomes continuous with the inter rod region [5].

Enamel is translucent but can vary in shade from yellow to grey. The colour of the tooth generally comes from the underlying dentin rather than from the enamel layer. Dentin is primarily yellow in colour, however if the enamel layer is thick and heavily mineralized, it obscures the yellow hue, resulting in a whiter tooth [5]. At the edges of the tooth, where no dentine exists, the teeth take on a bluish-white colour, given by the enamel. Although enamel structure is densely packed HA, some ions are able to permeate to varying degrees. Some ions occur naturally in the enamel layer [1]. We describe some of the most commonly found ions below.

2.2.3 Carbonate

The most prominent minor component of enamel is carbonate, generally located on a hydroxyl column or in a phosphate site. The substitution of carbonate does not fit well inside the HA lattice, leading to strain within the crystal structure and a more soluble material. In fact, carbonate is the first component of the tooth to be removed during an acid attack. It is more commonly found in the interior of the tooth, where it can reach up to 4% of tissue weight. It decreases closer towards the tooth surface (1% of the tissue weight). A schematic showing a map of carbonate distribution in typical human molar enamel is shown in Figure 2.4.

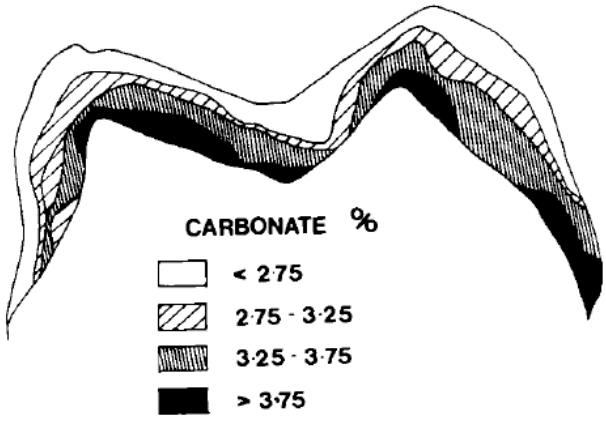

Figure 2.4: Map of carbonate distribution in typical human molar enamel [1]

2.2.4 Magnesium

Very little magnesium can be incorporated into the apatite structure as a substitute for Ca [23]. However, it has been found that higher levels of magnesium can be incorporated into carbonated HA due to the distortion of the lattice induced by carbonate formation [24]. Magnesium is also found on the surface of HA either as a hydration layer or as an absorbed overgrowth [1, 24]. The elemental distribution of magnesium throughout the tooth mirrors that of carbonate. At the surface, magnesium makes up about 0.1% of the total tissue weight and in the interior of the tooth, it is up to 0.3%. Figure 2.5 shows the typical distribution of magnesium throughout a human molar. As it has been previously determined that magnesium has difficulty substituting into the apatite structure, there is some support for the view that magnesium is located in the less well mineralized enamel and potentially in the organic matrix [1].

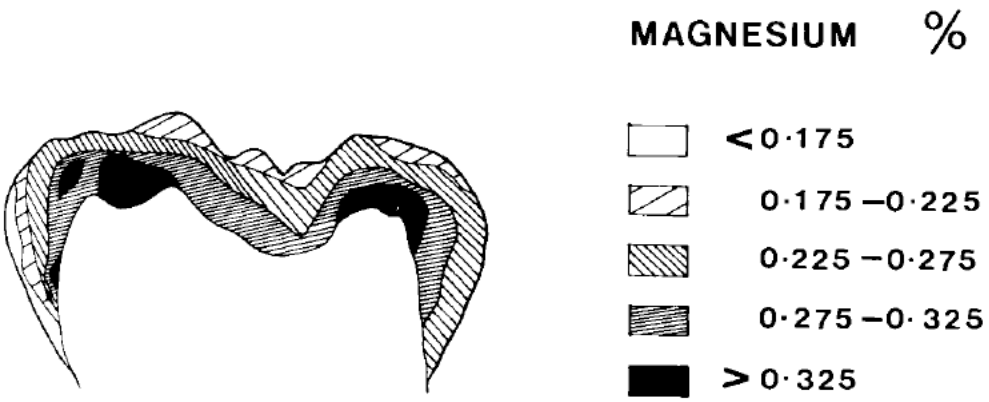

Figure 2.5: Map of magnesium distribution in typical human molar enamel [1]

2.2.5 Fluoride

In contrast to carbonate and magnesium, fluoride (F) fits well into HA structure. Unlike carbonates, F does not cause any significant defect in the crystal lattice. However, it does modify the crystal parameters by substituting for a column hydroxyl, giving rise to a reduction in crystal volume [25]. This modified structure is more stable than pure HA and is more resistant to acid attack [1]. In contrast to magnesium and carbonate, F is most commonly found on the surface of the tooth, with its concentration decreasing further into the interior of the tooth (Figure 2.6).

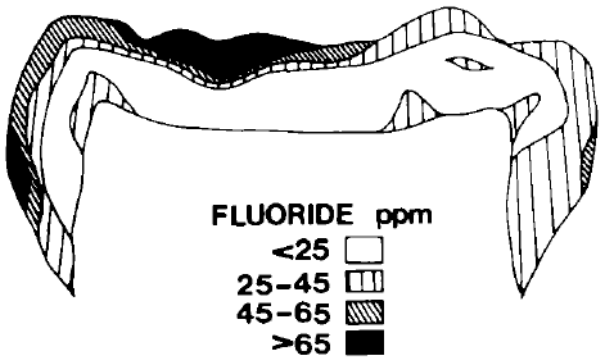

Figure 2.6: Map of typical fluoride distribution in human molar enamel [1]

F acquisition during enamel formation promotes the reversed distribution. It is initially incorporated into enamel during the secretory phase but is then largely lost before again being picked up during enamel maturation [1]. Over time, the F in the surface layer of the tooth will begin to be lost due to regular wear on the tooth. As F fits so easily and readily into HA structure, delivery occurs through a variety of methods such as fluorinated water, mouth washes and toothpastes as remineralization treatments [1].

2.3 Enamel Demineralization

2.3.1 Process of demineralization

The anatomical location of teeth places them in a unique position in the body, setting them apart from bones and other cellular tissue. The enamel layer is constantly exposed to food, drink, acidic environments, and bacteria [26]. These environments would result in drastic and rapid demineralization of bone and dentin in the same conditions. However, as the enamel layer is highly mineralized, it acts as a first line of resistance against demineralization processes that ultimately lead to the formation of cavities.

The primary method of enamel demineralization involves acid attack on and removal of the surface minerals from the enamel layer, allowing acid infiltration into the core of the tooth (Figure 2.7) [26]. While many ions are removed from the enamel surface during demineralization, the loss of Ca and P ions has the most significantly detrimental effect on enamel health [26].

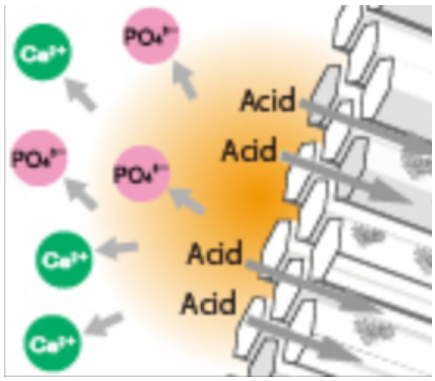

Figure 2.7: Schematic representation of enamel demineralization [27]

The baseline pH of the oral environment is in the range of 6.2-7.6, with an average pH of 6.7 [28]. Enamel will begin dissolve and demineralize at pH<5.5. The pH of the mouth can be drastically decreased through the consumption of acidic food and drinks and through microbial attack due to bacteria present in the mouth [26]. Figure 2.8 shows the results of acid etching on enamel at the same concentration found in food and drinks.

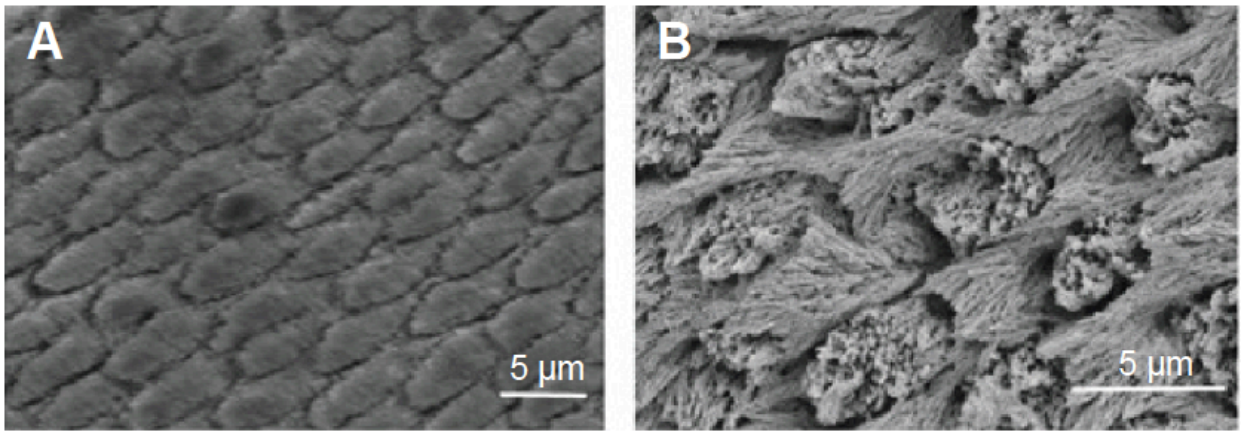

Figure 2.8: SEM images of (A) normal enamel, and (B) enamel etched with acid at the same concentration found in food and drinks [26]

The results of the demineralization process can range from increased dental sensitivity to the formation of cavities. Enamel is more susceptible to demineralization than HA due to the inclusion of impurities and ions that are not present in pure HA. For example, carbonates substitute in enamel for a phosphate ion in the crystal lattice. This creates a Ca deficient region on the surface of the tooth in addition to producing defects in the crystal lattice [29]. Such regions become softened and prone to collapse, resulting in cavity formation.

The bacteria in the mouth break down consumed sugars and carbohydrates and convert them to acid. Plaque on the surface of the tooth is capable of holding acid in close contact with the enamel surface for up to two hours before being neutralized by the basic conditions of saliva [29]. In the time that the plaque is acidic, ions in the tooth will be dissolved and leached out of the enamel layer. Repeated ingestion of sugars and carbohydrates combined with poor oral health will result in a significant loss of mineral from the surface of the tooth. The first visible sign of the repeated demineralization of the tooth surface is the appearance of white spot lesions [26]. The subsurface porosity caused by the demineralization of the tooth gives the lesion their milky appearance [30]. The maturation of white spot lesions can lead to a cavity through which bacteria can enter the interior of the tooth and destroy the inner structure [29]. Both the white spot lesions and resulting cavities can be seen in Figure 2.9.

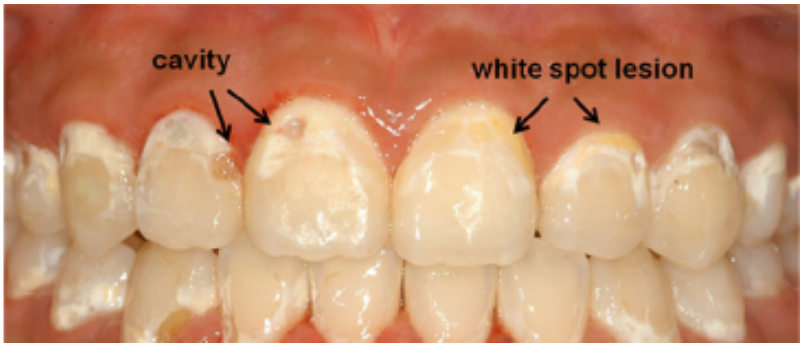

Figure 2.9: White spot lesions and cavities present on the surface of the tooth [31]

Research into demineralization has sought to link the chemical process of demineralization with the erosion of enamel. The chemical factors association with the erosion of enamel are related to the concentration of the acidic solution, the concentration of the Ca and P in the enamel, and the duration of the exposure to the acid solution [32]. One of the most commonly consumed acids is citric acid. It is present in everything from water, fruit, cheese and preserved/processed foods [33]. When the enamel surface is exposed to a citric acidic attack, the hydrogen ions in the solution directly attack the crystal surface, combining with the carbonate and phosphate ions that are being released, leading to direct surface etching. In addition, the citrate anions complex with Ca, removing it from the crystal surface [34].

The effects of citric acid go beyond stripping the mineral surface of Ca. Saliva naturally contains Ca that can be used as a first line of defense in tooth demineralization. However, after the consumption of foods or drinks that contain high levels of citric acid, up to 32% of the Ca in salvia can be complexed by citrate, reducing the amount of Ca making its way to the tooth surface [34].

2.3.2 Societal impact and economic cost

The main issue with enamel demineralization is the development of dental caries as a direct result of mineral loss. Globally, 60-90% of school children and 100% of adults have some degree of tooth decay [35, 36]. The World Health organization states that dental caries is the most common chronic disease worldwide and has been classed as a major global health challenge [35]. Although Canada is a global leader in oral health, an estimated 2.26 million school days are missed every year by Canadian children due to dental related illness [17]. Recent data from the Canadian government states that 39% of people, aged 12 and under, have had one or more permanent teeth affected by cavities [17]. This societal impact is broad, but the economic impact must also be considered. Globally, 5% of total health care expenditures relate to treatment of oral diseases [37]. This is estimated to translate to a direct cost in excess of USD $442 billion annually. In Canada, approximately 4.15 million working days are lost annually due to dental visits or dental sick-days [37].

Many governments around the world, including Canada, have recognized that enamel demineralization is a huge problem with far reaching social and economic repercussions. Dental research in recent years focuses on the prevention of demineralization and techniques to encourage enamel remineralization.

2.4 Remineralization and Prevention of Demineralization

2.4.1 Saliva

Saliva is constantly in contact with the enamel surface [4, 38]. Saliva acts in a dual role of protecting the enamel layer from erosive wear and as a first line of defense again demineralization. It can also partially act as a remineralization agent, but this has limited

efficiency. For erosive wear (demineralization that does not involve bacteria), the destruction of the enamel comes from the presence of acid from intrinsic or extrinsic means. Intrinsic sources relate to chronic vomiting and extrinsic sources relate to the consumption of acidic food and drink or acidic medication [38]. Saliva is useful in mitigating the effects of erosive wear on the tooth. It acts to dilute the acid in the mouth and also to eventually clear the acidic source from the mouth entirely. Additionally, saliva is a supersaturated solution, containing high levels of Ca and P. Bringing this supersaturated solution into close contact with slightly demineralized enamel can cause some degree of remineralization of the surface layer (Figure 2.10).

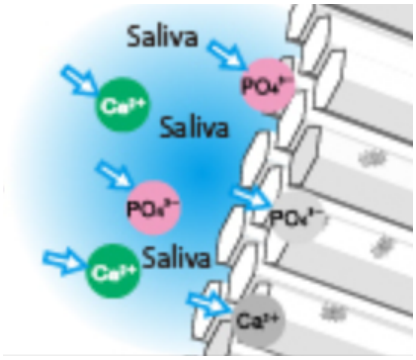

Figure 2.10: Schematic representation of enamel remineralization by saliva [27]

The significant of the degree of remineralization and hardening due to saliva is debated. Lippert *et al* examined the early stages of enamel surface dissolution and possible remineralization by saliva through atomic force microscopy (AMF) and nanoindentation [39]. Using these techniques, they measured the hardness of enamel at various stages of dissolution. They attempted to remineralize the surface of the tooth through immersion in simulated saliva and then again testing the hardness of the material. Saliva did not significantly remineralize the tooth as the hardness did not increase by a significant margin. However, they did show that teeth immersed in saliva were able to better withstand a future acid attack when compared to teeth that were not immersed in saliva [39].

2.4.2 Fluoride Treatments

The benefits of F treatments for oral health have been known since the beginning of the 20th century. F works to reduce enamel dissolution and promote enamel remineralization through the

formation of fluorinated hydroxyapatite (FHA), also referred to as fluorapatite [4, 40] (Figure 2.11).

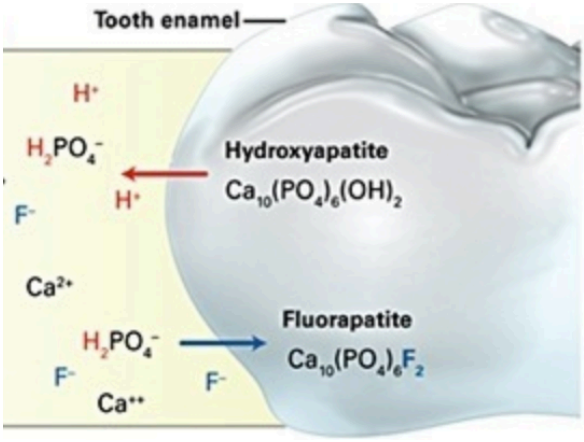

Figure 2.11: Schematic representation of fluoride ion infiltration into enamel layer

Work by Tanizawa *et al* showed that F^- ions easily exchanged with the OH^- ions in HA to form FHA. In low pH situations, CaF_2 was also produced [40]. The formation of FHA on enamel surface is promoted as the inorganic components of enamel are reactive due to their non-stoichiometry and the inclusion of impurities, such as carbonate groups [4]. Ingram and Nash examined the change in Ca:P ratio in three different Ca deficient HAs during an incubation with remineralization solutions containing 1, 2.5 and 5ppm F [41]. The resulting F-substituted HA offers a thermodynamically favorable location for dissolved Ca ions to re-enter the enamel crystalline lattice vacancies created by earlier acid attacks [41].

Based on these properties, F is used to control caries lesion development. Low levels of F in solution prevent enamel demineralization and promote surface remineralization though the enhancement of apatite deposition [4]. F can be introduced to the mouth through F containing toothpastes, fluorinated water, or mouthwashes. It deposits on the surface of the tooth through the formation F-substituted HA. This acts as a F reservoir which can release F to prevent demineralization during future acid attacks [4]. However, F is not a perfect long-term solution. Subsurface lesions treated by F are able to remineralize within weeks but years of F treatments are required for complete remineralization *in vivo* [42].

2.4.3 Calcium Treatments

While both Ca and P are integral to tooth health, Ca is more rapidly removed by demineralization and its loss has greater effect on the development of cavities [4]. In fact, findings have shown that Ca concentration in saliva is inversely proportional to cavity incidence [42]. Increased Ca concentration reduces the solubility of enamel and increases the drive for mineralization. Pearce and Nelson showed that use of a calcium chloride containing mouthwash led to a reduction in enamel porosity and an increase in surface hardness in acid softened samples [43].

2.4.4 Hydroxyapatite Treatments

Synthetic HA nanocrystals have biomimetic properties and easily substitute into natural enamel They contain similar carbonate concentrations and promote carbonate substitution onto the phosphate or hydroxyl groups [44]. The substitution of synthetic HA into demineralized natural enamel acts to remineralize the layer. Lelli *et al* examined a Zn-carbonate hydroxyapatite (Zn-CHA) containing toothpaste for remineralization and repair of the enamel surface. They looked at two groups of patients, one using the Zn-CHA containing toothpaste and the other using a sodium fluoride toothpaste. They found that the participants using the Zn-CHA toothpaste exhibited signs of superficial enamel repair via the formation of a protective carbonated HA coating [44]. Tschoppe *et al* also examined nano-HA containing toothpastes of varying compositions and with differing additions. They showed that pure nano-HA containing and $ZnCO_3$/nano-HA containing toothpastes significantly improved the remineralization of the enamel surface when compared to an amine-fluoride toothpaste control [45]. However, the topic of nano-HA and its role in improved remineralization is still contentious as there is evidence to point to nano-HA only being able to heal the surface layer of enamel and not the deeper parts of early lesions [4].

2.4.5 Calcium and Fluoride Combination Treatments

The benefits of F for oral therapy have been well recognized for many years. However, F alone has limited applications for sustained therapy as it is quickly removed from plaque and the oral cavity by saliva. In an effort to help plaque retain F for longer periods of time, combination therapies are examined. A clear linear relationship is established between levels of Ca and F in

plaque [46, 47]. By increasing the Ca concentration, plaque is able to retain larger amounts of F for longer times than would be possible otherwise. Adding Ca containing materials to F toothpaste can increase F retention. Hornby *et al* showed that a nano-HA containing toothpaste with sodium monofluorophosphate additions significantly reduced demineralization resulting from acid cycling of bovine teeth when compared to control samples [48]

The issues with current remineralization strategies in terms of long-term effectiveness and ability for deep tooth repair have highlighted the need for new materials that will be more efficient in promoting remineralization. Research has turned to bioactive materials, which by definition stimulate a positive response from the body [4]. Bioactive glasses are of particular interest for dental applications.

2.5 Bioactive glass

2.5.1 Background

Within the field of regenerative medicine, biomaterials that can replace or restore biological function are desirable. Many of the biomaterial options that are currently clinically available are, at best, biocompatible, meaning that they can be implanted in the body without harm to the living tissue [49]. However, this a far from perfect solution and does not allow for the implant or device to actively regenerate body tissue. As the research in this field progressed, people realized that there was a need for a new class of materials that interact positively with the physiological environment and eliciting a response from the tissue. Bioactive glasses fall into this category of bioactive materials. Bioactive glasses are a subset of glass-ceramic biomaterials that are surface reactive in physiological fluid. Upon immersion in said fluid, the glass will react and eventually, the glass surface will transform to produce HA, the inorganic precursor to bone. This process is shown in Figure 2.12.

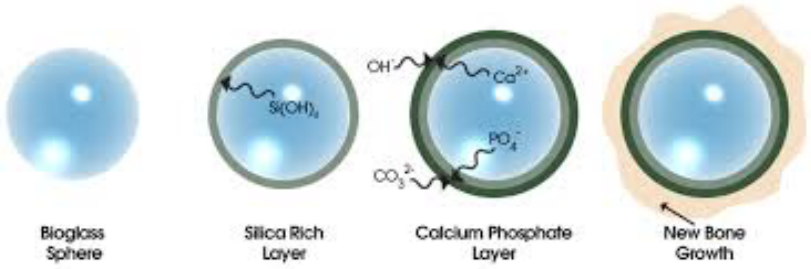

Figure 2.12: Schematic representation of the transformation of bioactive glass to hydroxyapatite [4]

Discovered by Dr Larry Hench in the 1960's, bioactive glasses have gone on to be investigated extensively for use as implant devices in the human body with the ability to replace and repair damaged or diseased bones, known as hard tissue engineering [6]. The glasses have also examined for use in soft tissue engineering applications such as wound healing [7, 50]. An additional benefit to bioactive glasses is they have antibacterial and antimicrobial properties due to the pH change that is inherent to the transformation from bioactive glass to HA [6].

The original bioactive glass composition is referred to as 45S5, a composition using 45 wt% SiO_2, and a 5:1 molar ratio of Ca to P. 45S5 is in a variety of applications from coating for implant devices to additions to toothpaste [51]. The composition of the glass has a great impact on the dissolution behaviour of the glass and the conversion time to HA. Therefore, the composition and molar ratios of the constituents are tailored to carefully suit the intended application. Metallic ions can also be incorporated into the glass [52]. These ions will be released during the transition process and careful selection of the ions to be included can lend additional properties to the restorative or wound healing application [53, 54]. The glass can be processed in one of two ways: melt derived or sol gel derived. Melt derived glass is the most common type of glass in general and is made by melting precursors in a crucible at high temperatures until a homogenous melt has been created that allows the formation of the glass network. The sol gel process is a more recent process in which liquid precursors are mixed at room temperature to form a glass network without the need for high temperature processing [8].

2.5.2 Uses of Bioactive Glass

Bioactive glass has been used for many applications since its invention. The most commonly used application is for hard tissue engineering, generally for the repair and regeneration of bone defects as a result of disease or trauma [55]. The use in load bearing applications is somewhat limited due to the inherent brittle nature of the glass. However, the incorporation of bioactive glasses into scaffolds has opened up further opportunities for them to be applied in load bearing conditions. For example, bioactive glass infused scaffolds are being researched for the potentially to regrow bone in areas that get very little oxygen, something that is a great clinical challenge with current technology [55]. Additionally, there is promising research that indicates that the incorporation of metallic ions into the bioactive glass could have beneficial properties ranging from increased mechanical properties to local antibacterial effects [56, 57]. In fact, the release of metallic ions has been shown to give rise to increased extracellular matrix mineralization, proliferation of osteoblasts, and the ability to combat osteomyelitis [50].

Figure 2.13 shows a tabulated list of the various bioactive glass inventions since its discovery in 1969 and their applications, showing the incredible variety of issues that bioactive glass can address.

Year (First Experimental Use)	Achievement/Application
1969	Invention of the 45S5 glass composition (45S5 Bioglass®)
1977	Treatment of ear diseases by using Ceravital® glass-ceramics (replacement of middle ear small bones)
1978	Ocular implant (biocompatibility with corneal tissue)
1985	Approval by Food and Drug Administration (FDA) of the first 45S5 Bioglass® implant (MEP® implant for middle ear ossicular repair)
1987	Treatment of liver cancer (radioactive glasses)
1988	Clinical use of the 45S5 Bioglass®-based Endosseous Ridge Maintenance Implant (ERMI) in human patients
1993	FDA approval of PerioGlas (45S5 Bioglass® particulate used for bone and dental repair)
1998	Peripheral nerve repair
1999	FDA approval of radioactive glasses (TheraSphere®) for cancer treatment
2000	Wound healing
2002	FDA approval of Medpor®-Plus™ (polyethylene/45S5 Bioglass® composite porous orbital implants).
2003	Antibacterial (Zn-containing) bone/dental cements
2004	Lung tissue engineering
2004	Use of mesoporous bioactive glass (MBG) as a drug delivery system
2005	Skeletal muscle and ligament repair
2005	Treatment of gastrointestinal ulcers
2010	Cardiac tissue engineering
2011	Commercialization of a cotton-candy borate bioactive glass for wound healing in veterinarian medicine. FDA approval is pending.
2012	Embolization of uterine fibroids
2012	Spinal cord repair
2018	Use of radioactive glasses (TheraSphere®) in patients with metastatic colorectal carcinoma of the liver

Figure 2.13: List of bioactive glass inventions and their applications [7]

2.5.3 Bioactive glass in Enamel Remineralization

As bioactive glass forms HA, it is a good candidate for enamel remineralization. One of the first applications of bioactive glass in the dentistry field was focused on the treatment of dental hypersensitivity [51]. This led to the development Novamin® (particle size is around 18μm), for use as an active repair agent in toothpastes. In its first uses, Novamin was used to mineralize tiny holes in dentine and reduce hypersensitivity [51]. Tai *et al* reported on a 100 participant study where volunteers brushed twice daily with a Novamin containing toothpaste over a six week period [58]. They found that the bioactive glass particles adhered to the dentine and formed a HA layer, blocking the tubules that lead to dental sensitivity. After six weeks, gingival bleeding and plaque growth reduced by 58.8% and 16.4% respectively when compared with control groups who had used normal toothpastes.

Although, when used in toothpaste form, bioactive glass particles do not have prolonged contact with the tooth surface, it is still able to stimulate long term repair of enamel [51]. Earl *et al* conducted in vitro trials where dentine was lightly etched to reveal tubules. Novamin was applied to the etched surface and left to sit for 24hrs. At this time, a HA layer covered the surface. Novamin stimulated the deposition of HA over the damaged dentine [59] (Figure 2.14).

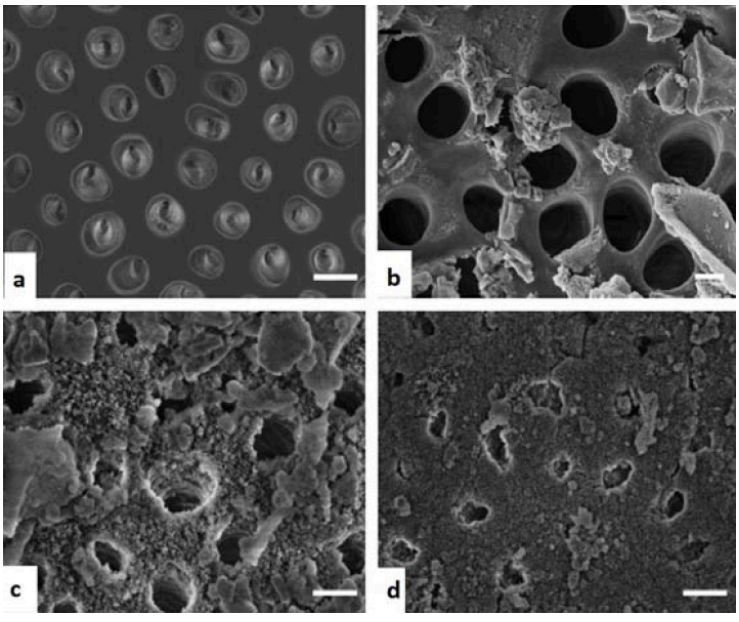

Figure 2.14: SEM images of human dentin (bar=1 micron) (a) untreated, (b) immediately after application of Novamin, after etching, (c) 24hrhs after Novamin application, (d) 5 days after application [59]

The knowledge that Novamin could be used to mineralize dentine was soon extended to enamel with the hopes of being able fully remineralize the enamel layer. Wang *et al* conducted the first study on the remineralization of enamel using bioactive glass. Teeth were artificially demineralized and then treated with Novamin or PerioGlass (particle size ranges between 90-710μm). Results showed that the smaller Novamin particulates more rapidly increased mineral content compared to the larger PerioGlass particulates [60]. Mehta *et al* compared the remineralization ability of Novamin and casein phosphopeptide-amorphous calcium phosphate (CPP-ACP). While both materials were able to remineralize early enamel caries, Novamin was able to perform remineralization much more effectively. Novamin also improved surface hardness when compared with CPP-ACP [61]. The potential of this technology was seen by the pharmaceutical giant GlaxoSmithKline who purchased it for use in their products in 2011. Novamin is now accessible to the consumer through Sensodyne Repair and Protect toothpaste products [62].

2.5.4 Transformation Mechanism of Bioactive Glass

When immersed in physiological fluid, bioactive glass undergoes a transformation to HA. The process of transformation is given in the following steps [11]:

Step 1: The rapid exchange of Na^+ with H^+ or H_3O^+ from solution

Step 2: The loss of soluble silica in the form of $Si(OH)_4$ to the solution, resulting in the breakage of Si-O-Si bonds and formation of Si-OH at the glass-solution interface: 2(Si-O-Si) + 2(OH^-) -> SiOH + OH-Si

Step 3: The condensation and repolymerization of a SiO_2 rich layer on the surface depleted in alkalis and alkaline earth cations: 2(Si-OH) + 2(OH-Si) -> Si-O-Si-O-Si-O-Si-O

Stage 4: The migration of Ca^{2+} and PO^3_4 groups to the surface through the SiO_2 rich layer forming a $CaO\text{-}P_2O_5$ rich film on top of the SiO_2 layer followed by the growth of the amorphous $CaO\text{-}P_2O_5$ rich layer by incorporation of soluble Ca and P from solution

Stage 5: The crystallization of the amorphous $CaO\text{-}P_2O_5$ film through the incorporation of OH- and CO^{2-}_3 or F^- ions from solution to form hydroxyl-carbonated apatite layer

2.5.5 Glass processing

Bioactive glass can be manufactured through two very different processing methods. The historical method of manufacturing bioactive glass is a melt derived process [7]. In this method, the precursors are added to a crucible and heated to high temperatures (over 1500^{o}C) for extended periods until a homogenous glass melt is formed [7]. The glass formers are the crucial components of the glass as they form the glass network. Silica is the most common network former [10]. As the melting point of silica is very high, it is necessary to add flux (Na_2O) to decrease melting temperature [10]. The final additions are fining agents, used to remove bubbles from the melt. Fining agents include potassium and sodium nitrates[10]. After formation of a homogenous glass melt, it is cooled, and the resulting glass monolith can be processed to the desired end shape. The overall process of melt derived glass making is shown in Figure 2.15.

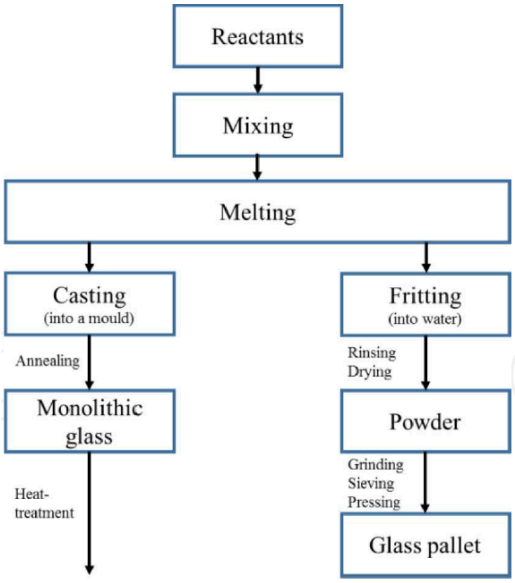

Figure 2.15: Schematic representation of melt derived glass making process [15]

Glasses made through a melt derived process have a fairly low surface area and low porosity. While different compositions are possible using a melt derived process, there are some limitations that are inherent to glasses made using this process. Firstly, the inclusion of metallic ions can be challenging as metallic precursors tend to oxidize during the extensive thermal treatment. Additionally, the compositional bounds in which a glass can be considered to be bioactive are somewhat limited. When looking at the traditional silicate-based system, melt

derived glasses have greatly reduced bioactivity when the silica content is increased above 60 mol% [7].

2.5.6 Sol-gel bioactive glass

Alternative processing methods for bioactive glass solved the issues with the melt-derived method. Sol-gel derived glasses are synthesised at room temperature using liquid precursors. The glass network, formed through hydrolysis and condensation reactions, results in a glass with very high surface area and porosity. The processing technique easily facilitates the introduction of metallic ions due to the ability to add them as an organic liquid precursor to the sol during the synthesis process [7]. The limitations with composition inherent to the melt derived process are overcome with sol-gel glass. Sol-gel glasses with silica content of up to 90 mol% are bioactive, opening up a whole new realm of compositions previously considered inert.

A sol is defined as a colloidal suspension of solid particles. In this suspension, the colloids exhibit Brownian motion, colliding within the medium [10, 63]. The gel is a rigid network of covalently bonded network formers creating a network with interconnected pores. Figure 2.16 shows a 2D representation of a random glass network. Within the glass network, bridging oxygens (BOs) link glass network-forming tetrahedra. Network modifiers are present as ions to alter the glass network and are compensated for by non-bridging oxygens (NBOs). The presence of network modifiers usually reduces the glass network connectivity through increasing the ratio NBOs to BOs [9].

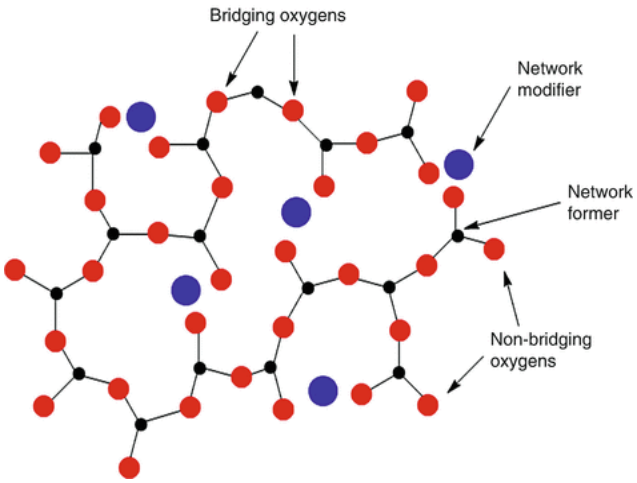

Figure 2.16: 2D schematic representation of glass network [7]

The sol-gel process has distinct steps to be able to create the final, desired glass. In the first step, the silicon alkoxides or organometallics precursors are mixed at room temperature to form a "sol" with the addition of deionised water. The ratios between water and precursors determines the composition of the glass [7]. The most commonly used silicon precursor, tetraethyl orthosilicate (TEOS), is insoluble in water but the presence of a catalyst can trigger hydrolysis of the precursors to form silanol groups [7]. Acidic catalysts result in higher fine-scale porosity development. Under acidic conditions (pH<2), $Si(OH)_4$ will come together, the silanol groups will condense and result in the formation of Si-O-Si bonds, thickening the sol to form a gel with water expelled as a by-product [10, 63, 64]. The process is shown in Figure 2.17.

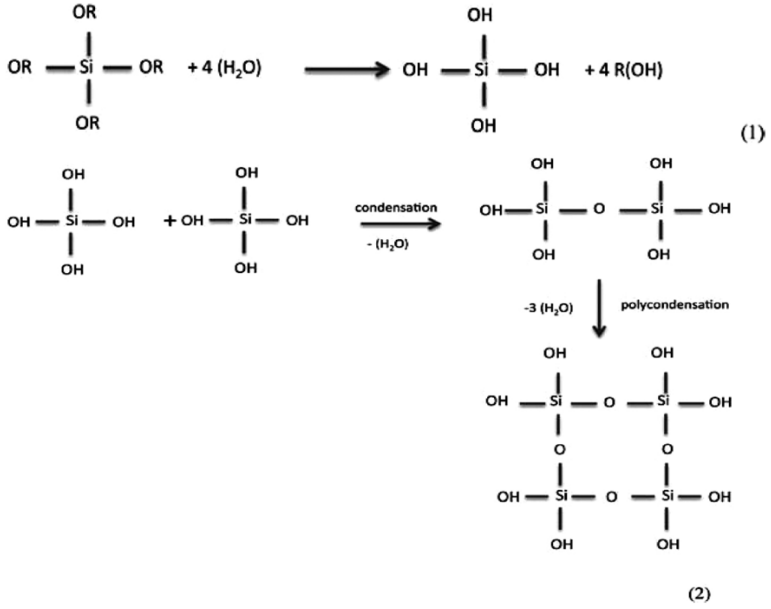

Figure 2.17: Process of glass creation through the sol gel method [15]

The gel is calcined to remove the remnants of the organic precursors that would otherwise contaminate the purity of the glass [10, 65]. The evaporation of water and alcohol leaves behind an interconnected pore network within the glass. These pores typically range in size from 1-30nm [7]. Figure 2.18 shows a schematic of the sol-gel glass synthesis process.

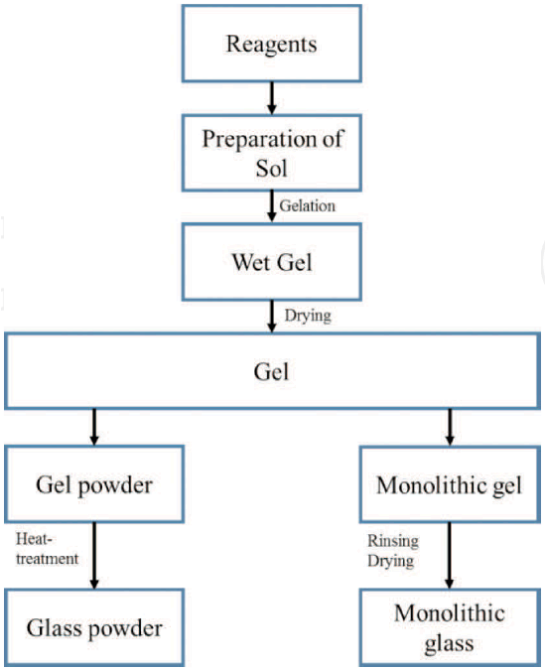

Figure 2.18: Schematic representation of sol gel glass making process [15]

The fabrication of crack-free monolith is challenging using the sol-gel method. Monoliths with dimensions exceeding 1 cm^3 are rare. The difficulty of formation increases with additions of any glass modifiers that alter the composition from pure silica [7]. Cracks appear during the drying process and occur mainly due to the large degrees of shrinkage in the network and the evaporation of the liquid by-products of the polycondensation reactions. As the vapors leave the glass, they must work their way to the surface through the interconnected pore network. This process may cause capillary stresses within the pores, resulting in cracking [7]. This makes sol-gel processed glass much more suited for powder, as the cracks that appear during drying are beneficial, making the grinding process easier. Additionally, the nanoporosities inherent to sol-gel glass facilitate grinding when compared to melt derived glasses [7].

2.5.7 Bioactive glasses for bone tissue repair

While this literature review has so far focused on dental applications for bioactive glass, there are wide ranging applications in the broader field of bone tissue engineering. Bone repair is a major and growing health concern due to an aging population [7]. Bioactive glasses bond with bone more rapidly than other biomaterials [11]. In fact, the discovery of bioactive glass has opened the doors to multiple new avenues of tissue regeneration, primarily due to its inherent

osteoconductive and osteoinductive properties [7]. A material that has osteoconductive properties encourages new bone to grow on the surface of the material, a phenomenon regularly seen in bone implants. Osteoinduction is the process by which osteogenesis is induced; a more active bone repair process involving bone forming cells called osteoblasts [66]. Osteoblast cells cultured on bioactive glasses produce collagenous extracellular matrix (ECM) that mineralizes to form bone modules, even in the absence of the usual supplemental hormones in solution [67].

It was initially thought that the formation of the HA was primarily responsible for the bioactivity and positive cell response seen for bioactive glasses [7]. However through in vivo studies we see that ion release from bioactive glasses is what stimulates osteoblast attachment and proliferation in addition to inducing angiogenesis [11]. As bioactive glass forms a HA surface layer, the glass releases dissolution products. These products have been previously shown to cause osteoblast gene up regulation for 45S5 [68]. There is increasing evidence to suggest that the ionic dissolution of inorganic components may be key to enhancing the bone restorative effect of glass [54, 69]. For example, Ca ion release has been shown to promote osteoblast proliferation, differentiation and ECM mineralization [70].

2.5.8 Metallic ions in bioactive glass

The ever-expanding applications for the field of bioactive glass has driven research to diversify available composition. There are limited numbers of network formers available; currently only silicate, borate, and phosphate based glasses are proving to be sufficiently bioactive options [10]. Therefore, the variability must come from another component of the glass and one area with promise is the addition of metallic ions to the glass structure. Many metallic trace elements already exist in the human body (i.e. Zn, Mg, Cu and Sr) and are known to have positive effects on bone metabolism. It is beneficial to include these ions into bioactive glass to have a controlled release at the desired site [10]. Other benefits of metallic ion inclusion in bioactive glass include osteogenesis, angiogenesis and antibacterial effects in the local physiological environment [10]. The benefits of several of the most common doped bioactive glasses are outlined below.

Magnesium Bioactive Glass

Magnesium is a naturally occurring element in the human body and is present in bone, dentin and enamel. It has been shown to have positive effects on wound healing, bone density and fracture resistance [10]. When incorporated into bioactive glass, magnesium can act as both a network former and a network modifier. When acting as a network former, it gives a reduction in strength of the Si-O-Si network bonds, resulting in a weaker glass network. With increasing magnesium concentrations, the degradation rate of the glass is decreased and can eventually hamper the formation of the apatite layer due to slowed reaction kinetics [10].

Silver Bioactive Glass

The addition of silver to bioactive glass provides increased antibacterial properties in the local physiological environment upon release into the wound or defect site [10]. With manipulation of the glass composition, there can be a prolonged and sustained release of silver ions while having no effect on the bioactivity of the glass [8, 10]. While the addition of silver ions is clearly beneficial for certain applications, it is also necessary that the amount does not go above 2wt% as that value has been shown to exhibit cytotoxicity [8]. Silver doped bioactive glasses are currently being explored for wound healing applications in addition to hard tissue engineering applications [10].

Zinc Bioactive Glass

Zinc is essential in the body where it acts as a cofactor for many enzymes, stimulates protein synthesis and aids in the growth and development of bone cells [10]. It also has antibacterial properties against certain bacteria. The introduction of zinc into bioactive glass has no negative influence on the bioactive behavior of the glass. In fact, certain zinc containing compositions exhibit higher surface area than their non-zinc containing counterparts, which has a positive influence on bioactivity [10]. When looking at the incorporation of zinc into the glass structure, it can act as both a network former and a network modifier. At low concentrations, zinc incorporates as a network modifier but as the zinc concentration increases, the zinc switches to act as a network former [10].

2.6 Introduction of metallic ions

The idea of ion treatments for enamel improvement is not a new concept. For example, this is why F is introduced to the oral cavity in most circumstances [41]. As F is not a long-term solution and does not give the best remineralization results, research in recent years has focused on the possibility of the inclusion of other ions in enamel to slow demineralization and enhance remineralization. One of these ion options is magnesium that already naturally occurs in enamel [1]. Magnesium has been successfully incorporated in HA via a variety of synthesis techniques [71, 72].

Other options include zinc and strontium, both of which occur in abundance in native enamel [1]. Mohammed *et al* showed that the introduction of zinc ions in enamel results in an inhibitory effect on enamel demineralization. Strontium is an interesting candidate as it is located just under Ca on the periodic table. As such, strontium may behave in a similar way to Ca in the enamel structure [73]. Wang *et al* showed that the addition of strontium ions to an acid solution can reduce the erosive impact of the acid solution on the enamel surface. The strontium ions form a layer on the surface, replacing Ca, that acts to protect the enamel from attack [73]. The substitution of Ca with strontium is also seen in the synthesis of synthetic Sr-substituted HA [74, 75].

Magnesium, strontium and zinc occur in abundance in native enamel (~600-2500 ppm)[1]. The effects of the more major inclusions have been extensively researched in recent years. Now, attention is turning to minor, trace elements also present in enamel. Ti is a less-researched trace element in enamel. However, it has been extensively researched as an additive to synthetic HA for a variety of biomedical applications for its ability to induce higher hardness, improved mechanical properties and antibacterial properties [13, 15, 76].

2.6.1 The presence of Ti in native enamel

Ghadimi *et al* explored the relationship between Ti and the physical properties of the enamel layer. They show that on average, Ti exists in roughly a 2-fold increased concentration in enamel

compared to the rest of the hard tissue in the human body [2]. Ti enters enamel through the consumption of gum or candies that contain trace amounts of Ti [77]. The typical exposure to orally introduced Ti for the average USA adult is on the order of 1 mg per kg of body weight per day [77]. Previous studies have placed the average Ti amount in enamel ranging from 10-200ppm [1, 2, 78].

Nineteen trace elements were found in native tooth enamel by Ghadimi *et al.* Concentrations of the various trace elements varied considerably among enamel samples, and were determined through ICP analysis [2]. Hardness was measured using Vickers microhardness measurements. Shade was determined by tooth spectrophotometry. Differences in crystallographic dimensions between the teeth with differing trace elements was determined using X-ray powder diffraction analysis. Teeth with a higher Ti concentration showed significantly decreased enamel crystal domain size through a smaller unit cell, increasing tooth hardness and higher lightness [2]. The decrease in crystal domain size relates to the smaller ionic radius of Ti^{4+} as it substitutes for Ca^{2+} within the HA crystallographic lattice, resulting in a decrease in cell parameters [13, 76, 79].

The physical changes produced by the introduction of Ti in enamel are desirable from a clinical point of view. A harder enamel layer would make the tooth more resistant to the stresses imposed by diet. Ti presence also correlates to higher tooth lightness, which is a goal that is often sought in clinic for aesthetic considerations. Despite all this, there is a general lack of research into the use of Ti in active remineralization agents. Previous research demonstrates synthesis of synthetic HA with Ti inclusion (TiHA), this may be a good model to understand the structural and biocompatibility changes induced by the introduction of Ti in dental enamel.

2.6.2 Titanium in synthetic hydroxyapatite

Ti is incorporated into synthetic HA by wet chemical processes, most commonly co-precipitation [14, 15, 80]. The production of synthetic TiHA has been of interest for the fields of bone tissue engineering and dentistry due to the ability of the material to integrate with host tissue [13, 14, 76, 81].

Characterization

Huang *et al* produced TiHA via a co-precipitation method. They synthesised TiHA containing 0, 0.8 and 1.6 wt% Ti. XRD was used for structural analysis, with all compositions exhibiting the expected major peaks for HA. No additional peaks that could be associated to the presence of Ti were seen for calcination temperatures up to 1000^{o}C. For calcination temperatures higher than 1200^{o}C, 1.6 wt% Ti HA showed calcium titanate peaks, indicating thermal instability. Raman analysis of all compositions showed only bands consistent with HA. Through TEM and XRD, they showed that the incorporation of Ti into the HA structure inhibited grain growth. Additionally, the HA grain size decreased with increasing Ti content [14].

Ergun synthesized Ti containing HA via a co-precipitation method [79]. Ti was substituted into HA at both 2 and 5 mol% Ca or P. This work also showed no evidence of Ti at low sintering temperature through XRD analysis. The unit cell volume of TiHA decreased with increasing Ti content. The grain size of HA decreased with Ti incorporation. However, after a certain limit, Ti ions promoted the decomposition of the HA phase and the formation of porosities in the material. Similarly to Huang *et al*, calcium titanate phases appeared after high temperature (>1100^{o}C) sintering. Bands associated with Ti phases (primarily $CaTiO_3$) also appeared with FTIR analysis above this temperature, specifically between 725-800 cm^{-1}, attributed to the presence of Ti-O bonds.

Ribeiro et al examined how the uptake of Ti ions in HA particles, through incubation of HA in Ti containing solutions, leads to changes in the FTIR spectra [81]. Once again, no bands associated with the presence of Ti were observed. However, there was indirect evidence of the structural changes that the uptake of Ti has on HA. Several parameter changes are consistent with the indication that there is a change in the orthophosphate ion in the presence of Ti. For low Ti concentrations, the phosphate ions in HA presented features like phosphate ions in well-crystallised HA. The bands at 3400 and 1630 cm^{-1} become more prominent with increasing Ti, suggesting the formation of a hydrated complex with increasing Ti. The spectra are shown in Figure 2.19.

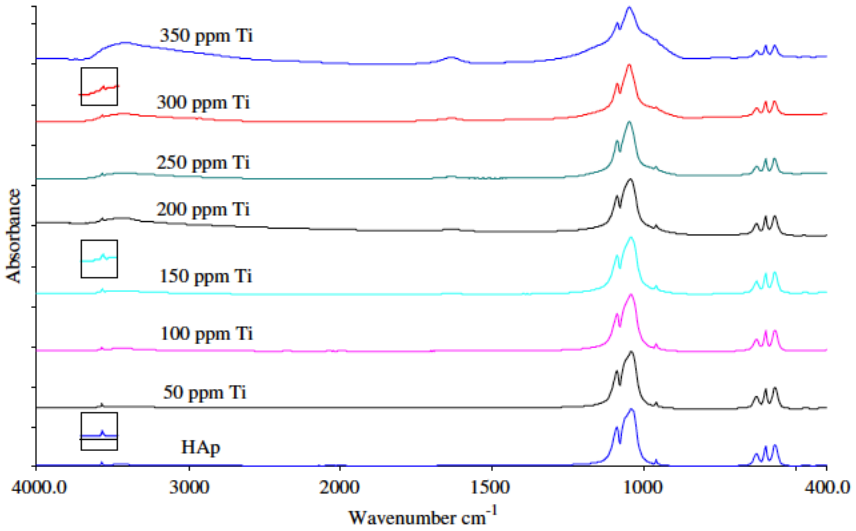

Figure 2.19: FTIR spectra of HA and HA powders after incubation in solutions with different Ti concentrations [81]

Cell Response

Ti inclusion in HA has an effect on the cell response to the material. As Ti implants and native HA have interfacial interactions, there was initial concern that atomic diffusion of Ti into HA could cause a toxic effect on the body or decrease osteoblast (bone forming cell) adhesion and proliferation [14, 16, 82, 83]. Ergun et al examined differences in human osteoblast adhesion between pure HA, Ti doped with HA, calcium titanate, and HA/calcium titanate composites [82]. Their results showed that osteoblast adhesion increased with greater Ti substitution into the HA lattice. Additionally, they found that osteoblast adhesion was almost 4.5 times greater for Ti containing HA over pure HA.

Huang et al studied the attachment of human osteoblast adhesion on Ti substituted HA [14]. TiHA showed high levels of human osteoblast cell attachment, with the cells maintaining their osteoblastic morphology. Ti substituted HA supported the proliferation of osteoblasts, and a larger amount of extracellular matrix was produced by the osteoblast cells when cultured on TiHA compared to pure HA. TiHA surface is preferred for the growth of osteoblast cells over pure HA.

2.6.3 Ti in Bioactive Glass

In an earlier section, we provide a brief overview of metallic ions in bioactive glass. The possibilities for inclusions are wide ranging but not all are commonplace. For example, the

inclusion of Ti in bioactive glass is not extensively researched. As Ti can act as a crystallization nucleator in amorphous materials, its incorporation in bioactive glass has posed potential issues. However, several studies have looked at Ti-containing glasses of various compositions and processing methods. Using primarily the melt-derived method, Ti-containing bioactive glasses have been made based on phosphate, silicate, and lithium borosilicate glass networks [84-88]. Wren *et al* saw disruption to the glass network with the introduction of Ti to Si-Ca-Sr-Zn melt-derived glass. The concentration of NBOs relative to BOs increased with increasing TiO_2 concentration, as Ti acts as a network modifier [87]. Concentration of Ti above 20mol% resulted in significant crystallization of the glass network.

Rodriguez *et al* examined Ti containing borate and silicate-based melt-derived bioactive glasses for the purposes of antibacterial coatings on metallic implants. The introduction of Ti did not significantly alter the solubility behaviour of both the silicate and borate-based glasses, up to 15 mol % Ti for the silicate glass and 10 mol % for the borate glass [86]. However, the inclusion of Ti did result in some degree of crystallinity for both the silicate and borate glasses, with the most crystallinity observed in the Ti-borate glasses. Ti was consistently released to solution throughout immersion in water, approximately 5ppm after 7 days of immersion. The borate glasses showed higher degrees of antibacterial behaviour compared to the silicate-based glass. However, this was attributed to the more rapid release of zinc, another antibacterial agent, from the more rapidly dissolving borate glass rather than the influence of the incorporated Ti. Both silicate and borate Ti-containing glasses induced a decrease in osteoblast cell proliferation as a result of contact.

Ni et al synthesised sol-gel derived bioactive glass 58S with Ti inclusion, based on a silicate network with additions of CaO, P_2O_5 and Na_2O [85]. The introduction of Ti did not result in major crystallinity. However, it did effect the dissolution behaviour of the glass, slowing it down compared to non-Ti containing glasses of the same composition. FTIR analysis of the mineralized glasses show indicators of HA formation after 5 days of immersion in simulated body fluid, although they are less pronounced for the Ti-containing glasses. No bands associated with a Ti

phase are observed. SEM analysis also showed that the appearance of morphology characteristic of HA was not observed on the surface of the glass until 5 days of immersion. Even after 5 days, the HA crystal morphology on the Ti containing glass was markedly different to the non-Ti containing glasses.

While studies have individually looked at the effect on structure, dissolution, mineralization and cell viability of Ti-containing bioactive glasses, the release of Ti to solution is not regularly reported and detailed analysis of the formed HA layer is not reported. Conversely, the idea of tailoring glass composition and dissolution behaviour to result in retention of the Ti within the glass network and eventual HA layer has not been explored. Furthermore, there are no cell culture studies on the effect of Ti inclusion in bioactive glass. Such studies are important to understand the biocompatibility of the glass for potential biomedical applications ranging from bone tissue engineering to enamel remineralization.

2.7 Conclusions

Dental enamel is the most highly mineralized material in the entire body. The composition of enamel is primarily inorganic crystalline HA (96%) and the remainder is an organic phase (4%). As enamel is not a living tissue, it cannot repair itself like other mineralized tissues in the body. Additionally, the working environment of the teeth place stresses upon them that are unlike anything else experience in the body. The acid environment caused by food and drink consumption and the constant wear that the tooth undergoes cause minerals to be lost from the tooth in the process known as demineralization [26]. Repeated and prolonged demineralization causes the tooth to lose its structural integrity, leading to the formation of dental caries. This ranges in severity from dental sensitivity to the loss of dental mass. In Canada and around the world, this is a large scale health issue that has huge societal and economic costs associated with it [17].

Current commercially available remineralization treatments such as F washes and toothpastes, and Ca treatments have some level of success but are not capable of completely and continually

remineralizing the enamel layer that is under constant stress from the local physiological environment [4]. As a result, research has turned toward new techniques such the use of bioactive materials.

In the area of bioactive materials, bioactive glass has been explored as a method for enamel remineralization. Bioactive glass is reactive in physiological fluid and has the ability to transform into HA [6]. Research shows that the use of bioactive glass greatly improves the remineralization ability the enamel layer when compared to current treatments [61]. Going beyond the remineralization of acellular enamel, bioactive glass demonstrates exemplary properties for regeneration of cellular physiological materials such as bone. The ions released by bioactive glass during dissolution and the formation of a HA layer work together to promote the attachment and proliferation of bone forming cells [8]. Metallic ions are already commonly included in bioactive glasses of varying composition, tailored to suite the specific, targeted application [9].

Ion inclusion research exploits the fact that many ions are found in native enamel. If the concentration of the ions can be increased or controlled, the structural properties of the enamel can be improved to reduce dissolution [4]. Ion inclusions that are being researched include magnesium, strontium and zinc [14, 71, 73, 89]. A less researched inclusion is Ti, which does not occur naturally in enamel but is introduced through the consumption of candy and gum [77]. The presence of trace amounts of Ti in enamel has been correlated with increased tooth hardness and brightness [2].

Ti containing bioactive glasses have not been extensively explored, even less so when we look at sol-gel derived glasses. The available literature on existing Ti-containing bioactive glasses does not provide a complete analysis of the material from structural to mineralization characterization in addition to cellular response.

A Ti-containing bioactive glass may be a suitable candidate for the remineralization of enamel. Clinically desirable properties are induced through Ti inclusion in native enamel. However, the

exploration of an active enamel remineralization agent with Ti inclusion has not been extensively researched previously. Going beyond the field of dentistry, a Ti containing bioactive glass could have implications for the broader field of bone tissue engineering if the same improved osteogenic response is seen for this material as is seen for synthetic HA with Ti inclusion.

Chapter 3: Synthesis, characterization, and in vitro investigation of sol-gel silicate-based bioactive glass with titanium inclusion

3.1 Introduction

Existing research on Ti-containing bioactive glasses has entirely overlooked the idea of tailoring glass composition and dissolution behaviour to result in retention of the Ti within the glass network and eventual HA layer, instead choosing to focus on targeting Ti release to solution. Previous work on synthetic HA with Ti inclusion show improved properties, ranging from better mechanical properties to increased osteogenic response. When we look at applications for this material, we see that trace amount of Ti in dental enamel improves its hardness and shade, leading us to our research question for this chapter: can we synthesize a Ti-containing bioactive glass that will mineralize to create a Ti-containing HA layer? In this chapter, we propose a method for synthesis of a Ti-containing bioactive glass (70STi) through the sol-gel process and conduct characterization on as-made (AM) glass to investigate the influence of Ti inclusion on glass structure. We also examine the bioactivity of the Ti containing glass in-vitro through characterization of mineralized glass as well as the Ti release behaviour in physiological fluid. For in vitro mineralization, we immerse the glass in simulated body fluid (SBF). SBF mimics the ion concentrations of human blood plasma [90]. This is an established procedure for bioactive glass mineralization tests [8].

Our Ti-containing glass is based off a previously well researched bioactive glass composition, 70S (70 mol % SiO_2 – 30 mol % CaO) [8, 91]. The binary 70S system is a simplification of the traditional quaternary glass network, removing sodium and P from the composition. This slows the reactivity of the glass when in physiological fluid, but the glass remains bioactive, particularly when produced through the sol-gel process that increases the surface area and porosity of the glass compared to melt derived methods. The simplified 70S base composition provides us with two advantages: Ti incorporation is more easily facilitated in simplified system due to reduced potential interactions; and the slowed dissolution rate allows to us to have greater control of Ti release behaviour.

For Ti inclusion, we target a 8 mol % (5 wt %) addition. Previous work on the inclusion of Ti in bioactive glass shows that small additions of Ti (under 20 mol %) do not nucleate significant crystallinities within the material [84, 85]. Furthermore, studies on the cellular response to synthetic HA with Ti inclusions show that inclusions under 10mol% result in the most favourable cellular response [14, 80, 82]. As such, we select a low Ti addition to optimize retaining an amorphous glass while creating a material that may induce the most favourable cellular response.

3.2 Experimental methods

Materials

Nitric acid (>99%), calcium nitrate tetrahydrate (>99%), tetraethyl orthosilicate (TEOS) (>99%) and titanium isopropoxide (>99%) are purchased from Sigma Aldrich (Canada).

Sol-gel processing

We fabricate a **70S** control glass (71.4 wt% SiO_2 - 28.6 wt% CaO) and **70STi** modified glass (71.4 wt% SiO_2-23.6 wt% CaO-5 wt% TiO_2)

We use all materials as received. We add Nitric acid to deionised water at room temperature in a Teflon beaker and magnetically stir for 5 minutes. Over a period of 5 minutes, we add TEOS dropwise and magnetically stir the solution for a further hour at room temperature. At this point, we slowly add calcium nitrate powder, allowing it to dissolve before the following addition and stir for a further hour. For the control glass 70S, we cast the resulting sol into polystyrene petri dishes and air dry at room temperature for 24 hours.

For the modified glass, we add titanium isopropoxide dropwise following the addition of calcium nitrate and subsequent stirring period. After the final addition, we mix the solution for a further 30 minutes or until the viscosity is too high for any further stirring. The sol is cast into polypropylene vials, sealed and stored at 37^{o}C for further gelation and aging for 48 hours. The gel is removed and placed in open petri dishes to air dry at room temperature for further 24 hours.

We calcine both the control and modified air-dried gels at 700°C. The temperature is reached at a heating rate of 3°C/min, followed by a 6-hour dwell time and cooled to room temperature. Following calcination, we manually grind and sieve the glass to isolate a particle size range of 25-45μm. We store the glass particles in a desiccator until analysis.

Particle characterization

We determine particle size (D50) of the sieved glass powders using a Horiba LA-920 (ATS Scientific Ink., Canada). The powders are dispersed in isopropanol before introduction into the machine. We perform three runs per powder sample.

The specific surface areas of the powders are measured with nitrogen gas adsorption and desorption isotherms collected using a Micrometrics TriStar II Plus 2.03 gas sorption system. Isotherms are analyzed using the Brunauer-Emmett-Teller (BET) method to understand surface area. Pore size is determined using the Barrett, Joyner and Halenda (BJH) method [92]. Prior to surface area measurements, the samples are degassed for 12hrs at 150°C under vacuum. Three runs are performed per powder sample.

X-ray diffraction

X-ray diffraction (XRD) diffractograms of the glasses are analyzed with a Bruker D8 Discover X-ray diffractometer (Bruker AXSS Inc., USA) with a CuKα (λ = 0.15406 nm) with power levels set to 40mV and 40mA. Three frames of 25° each are collected from 15-75° 2θ with an area detector and merged in post processing.

Fourier transform infrared spectroscopy

Fourier transform infrared spectroscopy (FTIR) is carried out on a Bruker Alpha II spectrometer, in ATR-FTIR mode, equipped with a deuterated-triglycine sulfate (DTGS) detector. The FTIR spectrometer resolution is set to 4cm^{-1}, the scan number to 128, and the scanner velocity is set to 10.0kHz. All samples were analyzed in powder form, placed directly on the spectrometer.

X-ray photoelectron spectroscopy

X-ray photoelectron spectroscopy (XPS) is carried out using a Thermo Scientific Kα spectrometer, equipped with an Al cathode with incident Kα radiation of 1486 eV and a spot diameter of 200μm. A low energy electron flood gun is used to prevent surface charging. Three points are selected for analysis for each sample. Data processing is performed using Avantage Software.

Inductively coupled plasma optical emission spectrometry

Release of Si, Ca, P, and Ti ions from the glass powders in simulated body fluid at several timepoints is measured using an inductively coupled plasma – optical emission spectrophotometer (ICP-OES, Thermo Scientific iCAP 6500, USA). Aliquots of 10mL are filtered through a 0.2μm nylon sieve and stored in 15mL falcon tubes. To each of these vials, 45 w/v% nitric acid is added and incubated at 60^{o}C for 2 hours. We analyse three samples for each timepoint and powder.

Scanning Electron microscopy

All samples are sputter coated (Edwards Auto 306 Cryo Evaporator) with a carbon coating (20nm thickness). Scanning electron microscopy (SEM) images of the surface of the materials are taken with a field emission SEM (FEI Inspect F-50) under an accelerating voltage of 5kV. Each sample is imaged in at least three different areas.

Bioactivity

The in vitro mineralization abilities of the control and modified glasses is examined with Kokubo's simulated body fluid (SBF) [90]. Glass is added to 50mL falcon tubes at a 1.5mg/mL glass to SBF ratio. Once a day, the vials are gently shaken to avoid agglomeration of the glass powder. Timepoints of 30 min, 1h, 6h, 1d, 3d, 7d and 14d are examined. Upon completion of the timepoint, the powders are rinsed with deionised water and then with 70% ethanol and dried overnight in an open falcon tube at 37^{o}C.

3.3 Results and Discussion

Sol-gel processing

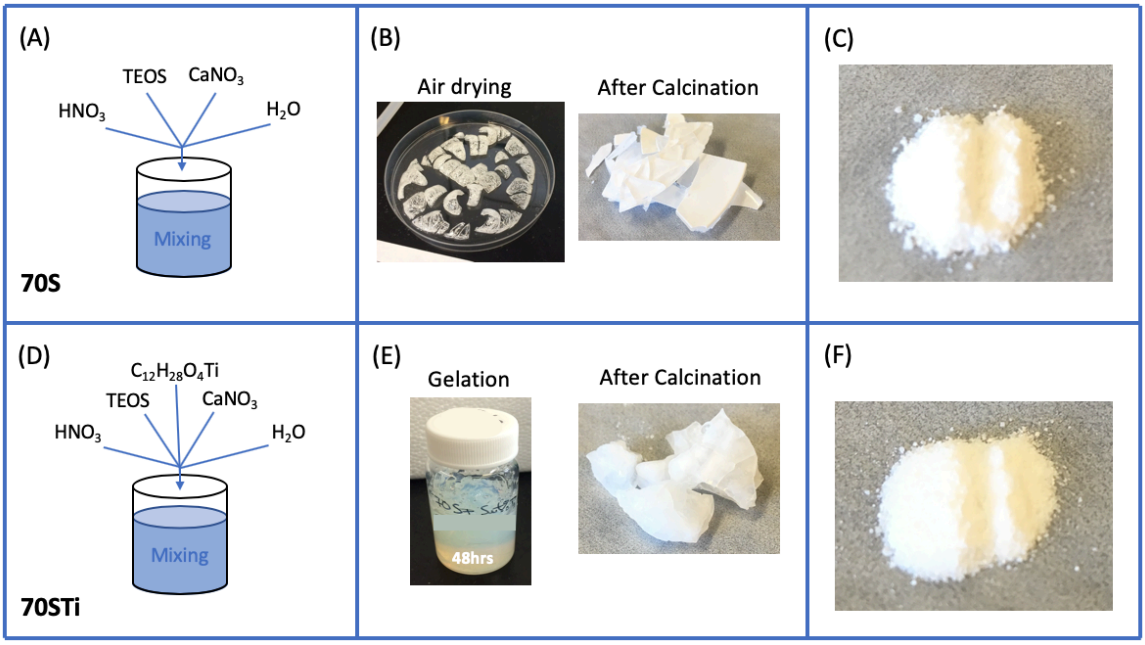

Figure 3.1: An overview of the sol-gel process for the synthesis of 70S and 70STi (A) 70S synthesis, (B) 70S drying and calcination, (C) ground 70S, (D) 70STi synthesis, (E)70STi gelation and calcination, (F) ground 70STi

Figure 3.1 gives an overview of the sol-gel process that was used to synthesize 70S and 70STi glass. Precursors are added to nitric acid and water, allowing for hydrolysis and polycondensation reactions to occur, forming 70S (Figure 3.1A) and 70STi (Figure 3.1D). 70S forms a very soft, pourable gel that dries clear (Figure 3.1B). 70STi gel is incubated at 37°C for 48hrs, to allow for increased interaction between the free Ti and the glass network during gelation. The resulting gel is opalescent (Figure 3.1E). After calcination, the 70S glass (Figure 3.1B) is brittle whereas the 70STi glass (Figure 3.1E) retains more of its shape in the form of large clumps. Finally, we manually grind and sieve 70S and 70STi to obtain particles in the range of 25-45µm. (Figure 3.1C and Figure 3.1F respectively).

Characterization of control and modified glasses

Figure 3.2A shows the FTIR spectra of the control 70S and modified 70STi glasses. Both glasses exhibit peaks characteristic of silicate-based glasses. Silicate groups can give peaks attributed to either bridging oxygen (BO) or non-bridging oxygen (NBO) groups. The peaks at 495cm^{-1}, 750cm^{-1}, 932cm^{-1} and 1030cm^{-1} can be assigned respectively to $\delta_{(Si\text{-}O\text{-}Si)}$, $\nu_{s(Si\text{-}O\text{-}Si)}$ of BO groups between tetrahedrons, $\nu_{as(Si\text{-}O\text{-}Si)}$ of NBO groups and $\nu_{s(Si\text{-}O\text{-}Si)}$ of BOs within the tetrahedrons [93-96]. The

spectra of 70S is consistent with those reported for glasses of the same composition and calcination temperature [91]. In 70STi there is no additional peak that can be attributed to the presence of a Ti species present in the glass structure. This mirrors previous work on the insertion of Ti ions into synthetic HA and bioactive glass, where the inclusion of Ti is not directedly observable in FTIR results [13, 14, 85, 97].

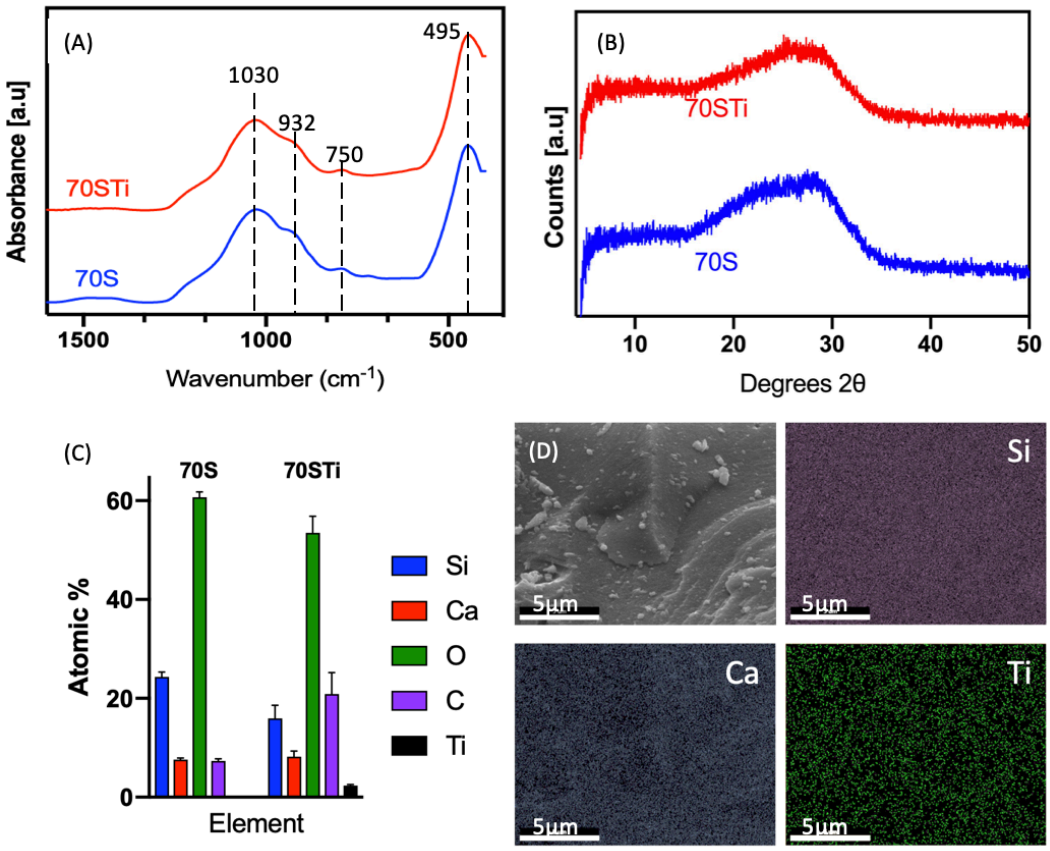

Figure 3.2: Characterization of as-made glasses. (A) FTIR analysis of glasses, (B) XRD diffractograms of glasses, (C) XPS analysis of surface composition, (D) EDS surface mapping of elements in 70STi

We perform XRD to determine if the introduction of Ti induces crystallinity in the material. While Ti can act as a nucleation point for crystallization within glass [98], our 70STi remains amorphous even after high temperature calcination, shown in Figure 3.2B. Both glasses exhibit the amorphous "halo" effect centered around 29° 2θ, characteristic of amorphous or highly disordered structures [99]. This contrasts to previous bioactive glasses with Ti inclusion, where crystallinity was nucleated through Ti introduction [86]. While crystallization of the glass does not prevent HA formation, it does slow it dramatically [6]. As we aim to produce the most bioactive glass possible, maintaining a fully amorphous glass is desirable.

Using FTIR and XRD, we are not able to directly observe Ti inclusion in the glass. However, we see Ti on the surface of all 70STi samples through XPS (Figure 3.2C), which shows 2.3 $\pm$ 0.01 at% Ti. The Si at% and O at% are significantly ($p<0.005$) higher for 70S compared to 70STi. The difference in Ca at% is not significant between the two compositions. EDS mapping (Figure 3.2D) confirms the homogenous distribution of elements throughout the material. Si, Ca and Ti are evenly distributed throughout the sample, which indicates that Ti is incorporated into the glass structure homogeneously and not agglomerated at certain points. EDS mapping of as made 70S is shown in Figure S1.1.

Particle size and specific surface area are important factors as they impact on the reaction kinetics once the powders are immersed in body fluids. The median particle size was consistent across both glasses, as shown in Table 3.1. The size distributions were also consistent (Figure S1.2)

*Table 3.1: Glass particle textural properties (n=3): average particle diameter, specific surface area (SSA), average pore width, and average pore volume, * p<0.02, ** p<0.0001*

Sample ID	Particle Size (μm)	SSA(m^2/g)	Average Pore Width (nm)	Average Pore Volume (cm^3/g)
70S	36 $\pm$ 3.8	69 $\pm$ 3.5 *	9.0 $\pm$ 0.1**	0.17 $\pm$ 0.01
70STi	36 $\pm$ 1.7	58 $\pm$ 4.9 *	10 $\pm$ 0.1**	0.16 $\pm$ 0.011

Representative N_2 adsorption isotherms for both glasses are shown in Figure S1.3. Both glasses show high specific surface area (SSA) values, comparable to previous sol-gel derived bioactive glasses [100, 101]. However, there is a significant difference in SSA between 70S and 70STi. 70S has a higher SSA (69 $\pm$ 3.5 m^2/g) than the modified glass (58 $\pm$ 4.9 m^2/g) (Table 3.1). This decrease in surface area could be attributed to the inclusion of Ti in the glass composition or to the extended gelation period of the modified glass. Extended gelation has been previously shown to reduce SSA [102]. The average pore size of 70STi (10 $\pm$ 0.1nm) is significantly higher than the

average pore size of 70S (9.0 ± 0.1nm). The difference in average pore volumes between the two compositions is not statistically significant.

Characterization of glasses immersed in SBF

The bioactivity of 70S and 70STi are investigated for up to 14 days in SBF (Figure 3.3). FTIR spectroscopy indicates HA formation after 3 days of immersion. In both glasses, there is an observable shift in the 1035cm^{-1} peak assigned to $\nu_{s(Si\text{-}O\text{-}Si)}$ of BO groups between tetrahedrons towards a broad band at ~1020cm^{-1}, assigned to $\nu_{(PO43-)}$ [20, 94, 95]. Additionally, a peak at 600cm^{-1}, 961cm^{-1} and a broader band at 1063cm^{-1} associated with the $\delta_{(PO43-)}$ are observed from 3 days of mineralization in both glasses [20, 94, 95]. The changes are not as defined for 70STi in the lower wavenumber range. The crystalline nature of the HA layer formed can be evaluated by the FTIR bands at 600cm^{-1} [103]. Over time, we see this band becomes well resolved into two distinct peaks, indicating that the developing HA is becoming more crystalline.

The band at 800cm^{-1}, associated with $\nu_{s(Si\text{-}O\text{-}Si)}$ [20], increases throughout immersion in SBF on both glasses, indicative of the formation of a silica gel layer on their surface.

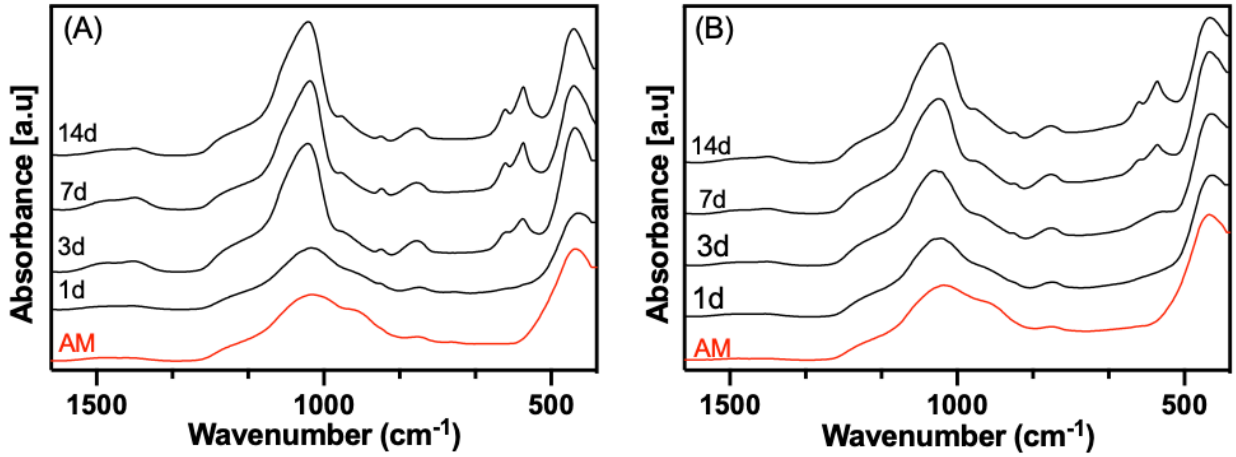

Figure 3.3: FTIR analysis of *glasses immersed in SBF: (A) control 70S, (B) modified 70STi*

After one day of immersion from 70S and 3 days for 70STi a peak at 870cm^{-1} appears. This is assigned to $\nu_2(CO_3^{2-})$, associated with carbonated apatite [104]. The broad bands at 1470 and 1425 cm^{-1} are attributed to the stretching modes, ν_1 and ν_3 respectively, of CO_3^{2-} [104]. All peaks and bands attributed to CO_3^{2-} and PO_4^{3-} become sharper and more defined with longer exposure

to SBF, indicating the formation of a calcium phosphate layer developing on the surface of the glass [9, 91].

While 70S presented more defined characteristic carbonate and phosphate indicators at earlier time points, the spectra for both glasses at 14 days of immersion are overall similar and exhibit equivalent peaks, although differences in HA crystallinity may exist. Several factors may delay the formation of HA on the modified glass at earlier timepoints: as shown in Table 3.1, 70STi has lower surface area than 70S. The reduced surface area of 70STi may result in slower HA formation compared to 70S [105]. Additionally, previous work indicates that the presence of Ti within the glass network alters its dissolution rate [85, 87]. Ti is a highly charged tetravalent cation, allowing it to act as both a network former and network modifier in the glass. When acting as a network former, Ti will disrupt the connectivity of the Si-O-Si network, creating additional BOs due to being the same valence as Si [85]. Additional BOs reduce glass solubility. When substituting Ti^{4+} ions for Ca^{2+} ions bonds, Ti-O bonds are formed with a more covalent character than Ca-O bonds [85].

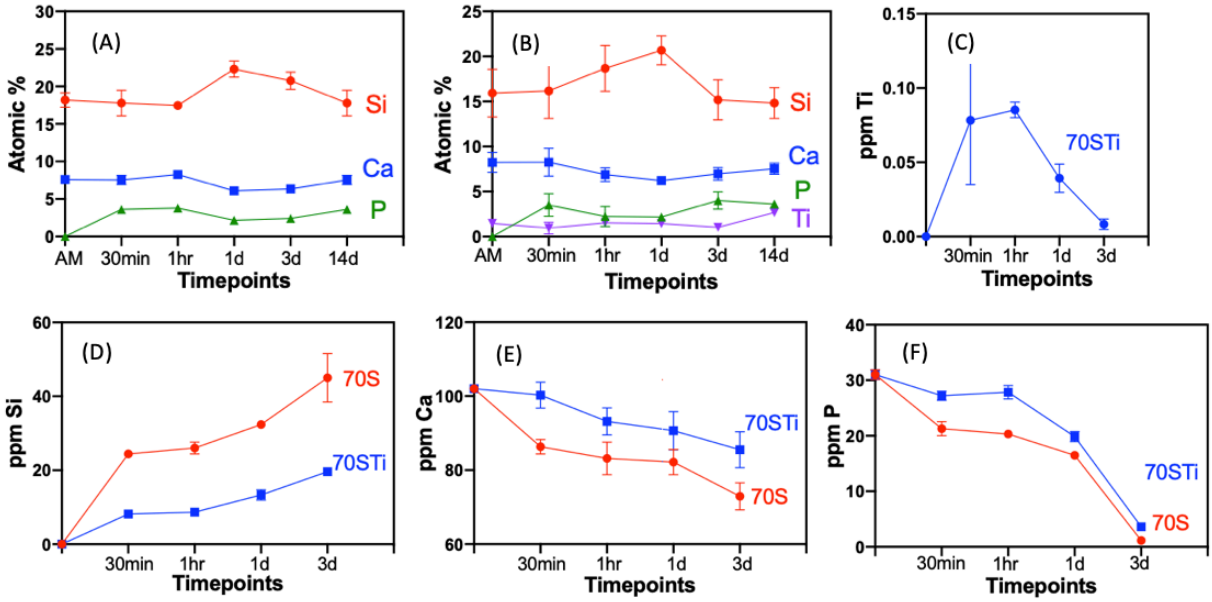

Figure 3.4: (A-B) Surface composition (atomic %) as obtained through XPS survey spectra for (A) 70S and (B) 70STi after immersion in SBF. (C-F) Elemental release from 70S and 70STi to SBF as obtained from ICP (C) Ti, (D) Si, (E) Ca, and (F) P

XPS analysis of the surface of the glass powders (Figure 3.4 A-B) confirms the formation of a calcium-phosphate rich layer after immersion in SBF. A strong indication for this is the presence

of P on the glass surface after immersion. For both 70S and 70STi, we do not observe any P on the surface of the AM glass, as it is not included in the composition. However, Ca and P appear after only 30 minutes of immersion for both samples, which indicates the initial stages of HA formation on both glass surfaces. Both Ca and P remain present and almost constant on the surface of both glasses for all later timepoints. From these results, we observe the gradual formation of Ca and P deposits on the surface of the glass, forming HA [106, 107].

Throughout mineralization, the amount of Si on the surface of the glasses fluctuates. Figure 3.4A, Si at% on 70S does not significantly change from the AM value (18 ± 0.95 at%) until one day of immersion when it increases to 22.31 ± 1.08 at%. There is not a significant change in Si at% between 1 day and 3 days of immersion. However, by 14 days of immersion, Si at% has fallen significantly to 18 ± 1.7 at%. We see a similar trend for 70STi (Figure 3.4B). There is no significant difference in Si at% until 1 day of immersion, going from 15 ± 2.7 at% for the AM glass to 21 ± 1.6 at% after 1 day of immersion. Between 1 and 3 days of immersion, there is a significant decrease to 15 ± 2.2 at%, with no significant change up to 14 days of immersion. The trend of increase and then decrease in Si content observed for both glasses is consistent with previous works that show the formation of a silica rich layer during the first stage of the reaction which is then covered by a HA layer at later timepoints [108]. The formation of this silica rich layer was already indicated by FTIR analysis, through the evolution of the band at 800 cm^{-1} as previously discussed. Changes in surface composition with respect to Si, Ca and P at% confirm previously reported results of HA evolution on the surface of bioactive glass [107].

Ti is observable on the surface of 70STi at every timepoint (Figure 3.4B), implying that it is present in the as-made glass and in the eventual HA that begins to form after 3 days of immersion. There is no significant different in Ti at% between the AM glass and the glass after 3 days of immersion. However, between 3 and 14 days of immersion, there is a significant increase in the amount of Ti on the glass surface, which seems to indicate accumulation of Ti on the HA layer formed on 70STi. This observation is new compared to what previously reported for Ti-containing bioactive glass, since previous work did not analyze the amount of Ti retained in the glass and measurable

on the surface before or after immersion, and just focused instead on the amount of Ti released to solution [85, 87].

We show Ti release to SBF in Figure 3.4C. At time zero, we do not detect Ti in solution as Ti is not inherent to SBF. After 30 minutes of immersion, 0.07 ± 0.04 ppm of Ti are released into solution. By 3 days of immersion, the levels of Ti released significantly decreases as the level approaches zero. We did not continue measuring after 3 days because SBF was refreshed after this time.

Ti release at all timepoints is very low, indicating that most of the Ti is retained within the glass initially and then within the calcium phosphate layer at later timepoints. Previous bioactive glass compositions that included metallic ions saw an increased release of metallic ions to solution over time [69, 109, 110]. More specifically, studies on Ti inclusion in bioactive glass show prolonged and increasing release of Ti for up to 30 days immersion in SBF, in contrast to the decreasing trend seen for our composition [86]. In literature, silicate-based glass with a similar Ti addition, release Ti to SBF up to amounts of around 4ppm after 30 days of immersion, an order of magnitude higher than the Ti release seen for 70STi [86]. We hypothesize that our glass retains Ti for two reasons. The high silica content of our glass slows the transformation to HA, allowing more time for Ti to integrate in the forming HA rather than release to solutions. Additionally, our sol-gel processing includes a 48hr gelation step. This extended gelation is absent from other sol-gel based Ti bioactive glasses. This allows Ti to have greater interaction with the glass network before drying and calcination, improving Ti retention in the glass and eventual HA layer.

Beyond looking at Ti release to solution, ICP analysis is a valuable secondary method to confirm the formation of HA on the glass. In Figure 3.4D we see the release of Si is from the glass to SBF across all time points, with increasing Si concentration in solution over time. 70S consistently releases more Si over three days of immersion compared to 70STi: by 3 days of immersion in SBF, 70S released 45 ± 6.6 ppm Si into solution. By the same timepoint, 70STi releases 20 ± 0.3 ppm Si. The release of Si to solution is an indicator of glass network dissolution and has previously

shown to be a reliable indicator of bioactivity [100]. The lower release of Si in 70STi is consistent with its slower reactivity compared to 70S, as shown by FTIR and XPS.

Ca release for 70S and 70STi is similar across all timepoints (Figure 3.4E). At 0 minutes, we plot the baseline concentration of Ca in SBF, with the values at all other timepoints showing the released Ca in addition to the Ca in SBF. As the glass network breaks down, Ca ions from the glass will be released into solution. However, in parallel with this, Ca is drawn from solution to reprecipitate on the surface of the glass, to form HA. As such, a decrease in Ca in solution is a good indicator of bioactivity in glass [100]. For 70S, there is a significant decrease in Ca release after only 30 minutes. The decrease from the baseline Ca concentration for 70STi is not significant until 1hr of immersion. For both compositions, there is no significant change between 1 hour and 1 day of immersion. 70S shows a further significant decrease from 1 day to 3 days. This period does not see a significant decrease for 70STi. 70S draws a significantly higher amount of Ca from solution compared to 70STi. This is consistent with the observed results from XPS and FTIR that indicate while that both glasses form HA, 70S does this at a faster rate, due to increased bioactivity compared to 70STi.

Similarly to decreasing levels of Ca in solution, decreasing levels of P in solution are an indicator of bioactivity and HA formation [100]. As before, the P ppm level at 0 minutes is the measure of inherent P in SBF. As P is not inherent to our glass compositions, no P will come from the glass itself, instead being drawn from SBF to the surface of the glass to combine with Ca to form HA. We observe a decrease in P ppm in solution for both glass compositions over time (Figure 3.4F). 70STi draws significantly less P from solution for immersion times of up to 1hr compared to 70S. This indicates a slower HA formation rate at early timepoints, as previously seen by FTIR and XPS. By 1 day of immersion, the difference in P levels in solution between 70S and 70STi is no longer significant. By 3 days of immersion, the concentration of P in solution for both 70S and 70STi converge to approximately 2 ppm.

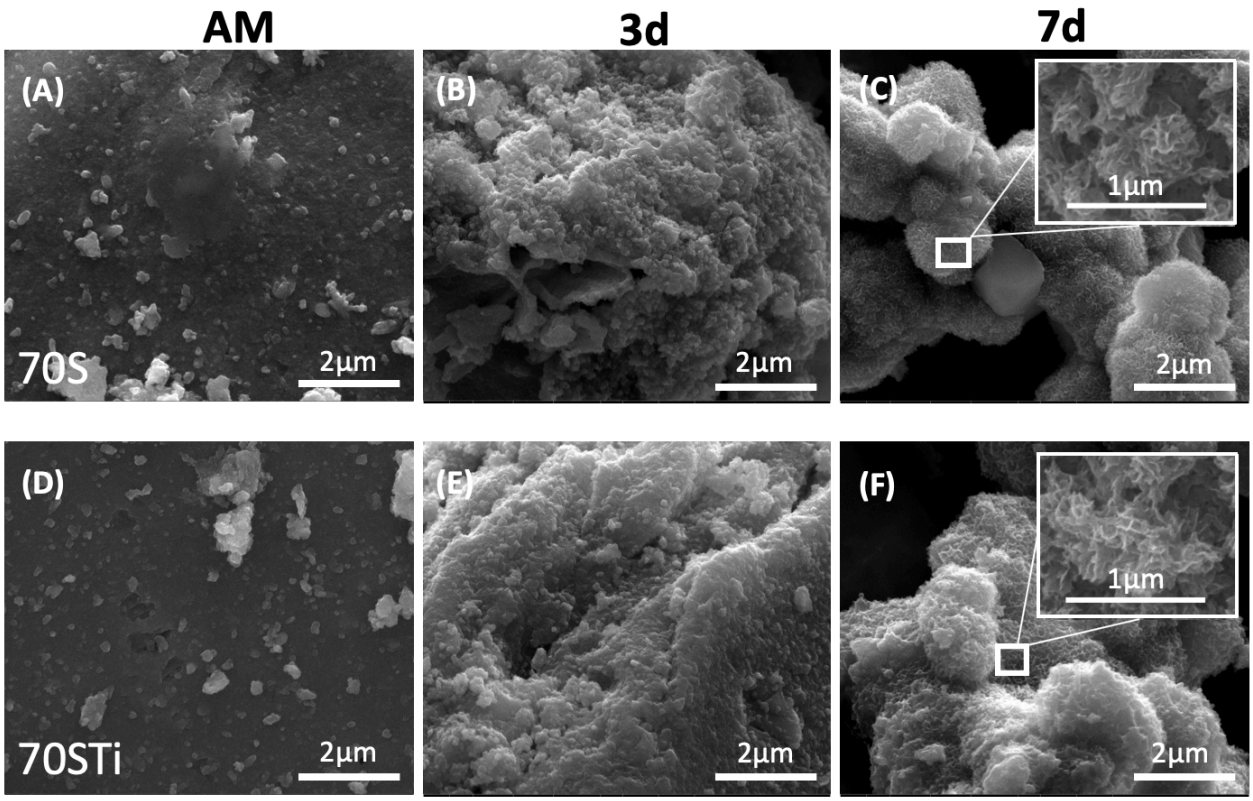

Figure 3.5: SEM Morphological characterization of 70S and 70STi as a function of time in SBF: (A) 70S AM, (B) 70S 3d immersion, (C) 70S 7d immersion, (D) 70STi AM, (E) 70STi 3d immersion, (F) 70STi 7d immersion

The formation of HA is also confirmed by SEM (Figure 3.5). The AM glasses are relatively smooth, with smaller particles adhered to the surface of the larger particles (Figure 3.5 A and D). There is no significant difference in appearance between 70S and 70STi. After 3 days in SBF, the surfaces of the glasses are considerably coarser. The smaller particles that are present for the AM samples are no longer present after three days, likely having been washed off by immersion in SBF. Additionally, a roughened surface is observed on both glasses. The surface of 70S (Figure 3.5 B) appears more roughened than 70STi (Figure 3.5 E), echoing our previous observations from FTIR, XPS, and ICP that 70STi is slower to develop HA.

By 7 days in SBF (Figure 3.5 C and F), the surfaces of both glasses are fully covered by developed flakey crystals, arranged in larger globule-type structures. This morphology is an indicator of HA formation [93]. There is no significant difference between 70S and 70STi by 7 days. This contrasts to previous work on Ti-containing bioactive glass where the morphology of the developed HA was significantly different to the HA on the surface of unmodified glass, showing this difference

after only 3 days of immersion in 1xSBF: HA crystals on the Ti-containing glass were arranged in worm-like patterns between 3 and 5 days of immersion rather than the globule morphology seen on 58S unmodified glass [85]. The change in morphology and mineralization behaviour seen in previous work impacted the degree of mineralization achieved. Timepoints up to 5 days of immersion for 58S with Ti inclusion did not reach the same degree of mineralization as unmodified 58S, unlike our results [85].

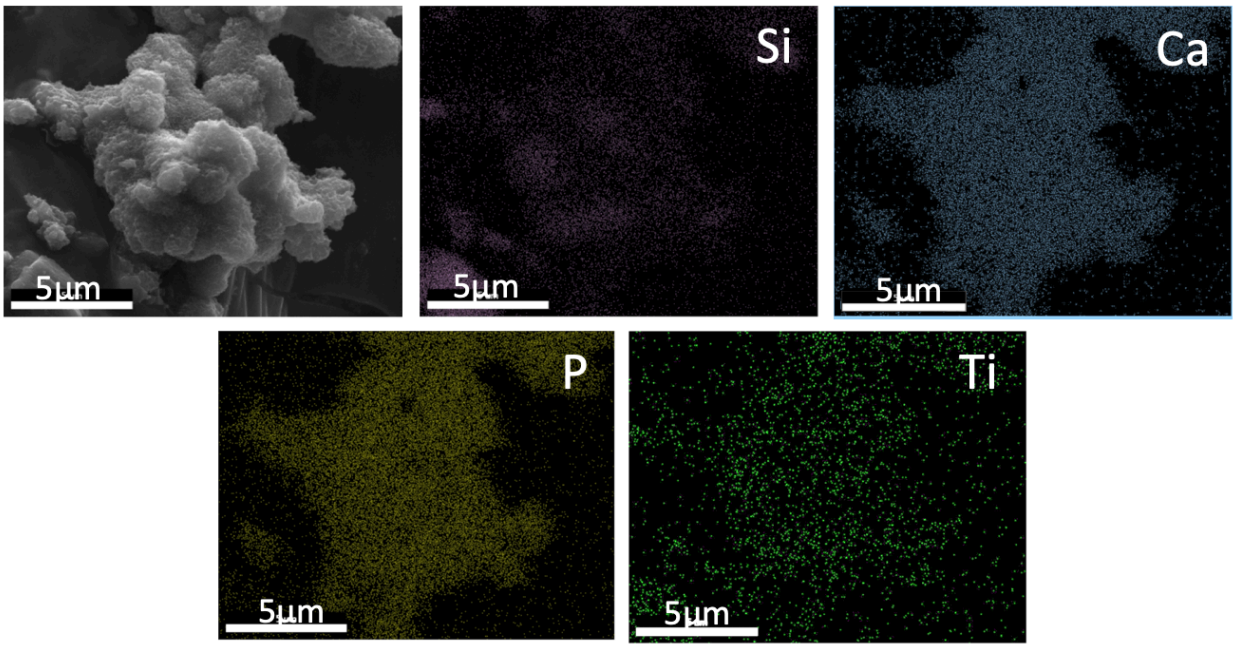

Figure 3.6: Elemental mapping of 70STi after 7 days of immersion in SBF

In Figure 3.6, we show the elemental mapping of 70STi after 7 days of immersion in SBF. The Si signal is weaker when compared to that for the AM glass (Figure 3.6), as the HA layer grows over and covers the silicate glass. Ca and P are distributed evenly across the material. The uptake of P indicates the formation of the calcium phosphate layer. Ti mapping indicates that Ti remains present during immersion in SBF and remains evenly distributed throughout the material. These results suggest the formation of Ti containing HA layer on the glass surface, confirming our previous characterization. Figure S1.4 shows the elemental mapping of 70S after 7 days of immersion in SBF for comparison.

3.4 Conclusions

In this chapter, we discuss sol-gel synthesis and characterization of a Ti containing silicate-based bioactive glass, 70STi. 70STi remains fully amorphous after calcination and exhibits high surface area. Using EDS and XPS, we confirm the presence of Ti in the AM glass. 70STi is bioactive, reacting in SBF to show clear indicators of calcium phosphate formation after three days of immersion. Very little Ti is lost to solution after immersion in SBF, and the presence of Ti is observed on the surface of the material at all timepoints during the formation of the HA layer. This indicates that the Ti is retained within the glass and results in the production of a Ti substituted HA layer.

This material is a good candidate for an enamel remineralization agent. Bioactive glass is already commercially available for this purpose. Incorporating Ti in the bioactive glass and through mineralization, in the HA layer, gives this material new, as yet unexplored functionally. Ti is already shown to influence the properties of native enamel to improve clinically desirable properties. In our future work, we plan to use 70STi as an active repair agent for enamel remineralization. Varying Ti addition to 70STi should also be explored. Compositions with higher and lower Ti additions are interesting to see how the incorporation in the glass network and HA layer changes with amount.

This chapter completes two of our stated research goals; (1) to fabricate a Ti-containing sol-gel bioactive glass, and (2) to examine the differences in surface area, reactivity and bioactivity induced by the inclusion of Ti in 70S. This leaves our third research goal; to investigate the effect of Ti inclusion in bioactive glass on cell viability and osteogenic differentiation. In Chapter 5, we will examine this objective.

Chapter 4: Investigation of cell response to sol-gel silicate-based titanium containing bioactive glass

4.1 Introduction

In Chapter 4, we outlined the synthesis and in vitro characterization of 70STi, a silicate-based sol-gel bioactive glass with Ti inclusion. Based on our review of literature, Ti-containing synthetic HA shows an increased cell response in terms of osteogenic differentiation [14, 16, 80]. This motivated us to examine the cellular response promoted by contact with 70STi. As enamel itself is acellular, we needed to choose which cell type to perform these experiments with. We selected human dental pulp stem cells (hDPSCs) to remain consistent with the potential dental application of this material. Additionally, hPDSCs exhibit rapid differentiation and can be easily triggered to undergo osteogenic differentiation if exposed to the correct media [111, 112]. They are extensively characterized for osteoblastic potential in vitro and in vivo, which makes them an excellent cell source for bone tissue engineering applications.

We conduct two experiments using 70S and 70STi to establish a complete picture of the cellular response: a cell viability experiment and an osteogenic differentiation experiment. 70S has been previously shown to have no negative effect on cell viability, so this will provide a useful baseline to examine the effects of Ti addition [113]. Furthermore, bioactive glass inherently promotes an osteogenic response due to ion release to the local physiological environment [8, 69]. However, we see in literature that the osteogenic response to Ti-containing bioactive glass is not researched. If our results were to show that 70STi has no negative effect on cell viability and promotes higher levels of osteogenic response than 70S, 70STi would have wide ranging applications across the field of tissue engineering.

4.2 Experimental methods

Cells

The human dental pulp stem cells (HDPSCs) are collected from permanent teeth and used at passage 3 to 6, as previously described [111]. The cells are cultured in α-MEM supplemented

with 10% (v/v) fetal bovine serum (FBS) and 1% (v/v) Penicillin/Streptomycin. They are incubated in a vented petri dish at 37°C, 5% CO_2 until 90% confluence. Cells are then trypsinized, counted and seeded into 96 well plates (3000 cells/well). For both the cell viability assays and osteogenic assays, the experimental set was as shown in **Error! Reference source not found.**.

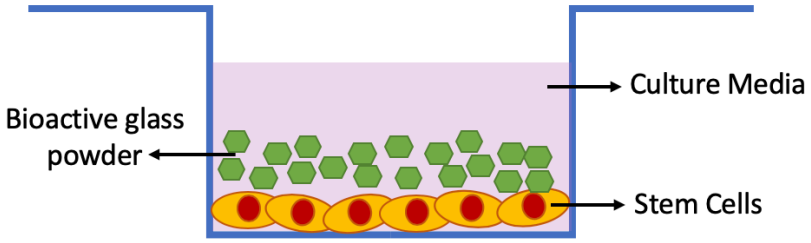

Figure 4.1: Experimental setup for cell experiments

Bioactive glass powder preparation for cell experiments

70S and 70STi are prepared as described in Chapter 3. For all experiments, the glasses are used as made. Before contact with cells, the glasses are sterilized by immersion in 100% anhydrous ethanol for 20 minutes. Following this, the excess ethanol is removed, and the glass is left to dry overnight in a biological safety cabinet.

Cell Viability

The cells are put in contact with 1mg bioactive glass/well. At designated timepoints (1d, 2d, 3d, 4d, and 5d), the cell media is aspirated from the well plates. 150μL of α-MEM supplemented with 10% (v/v) fetal bovine serum (FBS) and 1% (v/v) Penicillin/Streptomycin with a further addition of 10% (v/v) Alamar Blue is added to each well. 3 wells for each timepoint are used without cells as a blank. Following incubation of the well plate 37°C for 24hrs, 100μL of the reaction product is transferred to separate, flat bottom 96-well plate. The absorbance of Alamar Blue is read using a microplate reader (FLUOstar Omega, BMG Labtech). Increasing absorbance indicates increasing cell viability.

Alkaline Phosphatase Activity

The effect of 70S and 70STi glass powders in contact with HDPSCs was assessed based on alkaline phosphatase (ALP) activity. Cells are seeded into wells of a 48-well plate at 3000 cells/mL and

cultured for 4 days until confluent. The respective glass powders are then added (2mg/well) and incubated at 37^{o}C for 10 days. The cell plates are removed from the incubator and placed on ice to cool. The media is aspirated, and the cells are washed 2-3 times with ice cold washing buffer (20mM Tris-HCL). The washing buffer is aspirated and the ice-cold cell lysis buffer (20mM Tris-HCL, 200mM NaCl, 2.5mM MgCl2, 0.05% Triton X-100) is pipetted vigorously over cells then repeatedly up and down 20 times to burst and detach the cells from the plate. The lysate is collected in 1.5mL tubes on ice and then centrifuged at 4^{o}C for ten minutes at 15,000xg. The resulting supernatant is used to measure ALP activity with the LabAssay ALP KIt (Wako Chemicals).

4.3 Results and Discussion

Error! Reference source not found.2 shows cell viability results for AM 70S (1mg/well) and 70STi (1mg/well) in contact with hDPSCs for timepoints up to 5 days. We also show results for control cells, which are hDPSCs grown on tissue culture polystyrene without contact with either bioactive glass. Between day 1 and day 5 there is a statistically significant increase ($p<0.04$) in absorbance in the control, 70S and 70STi wells indicating continued and sustained cell viability as the hDPSCs proliferate. In Chapter 4, we saw that 70STi releases small amounts of Ti to solution at early mineralization timepoints. However, we see from Figure 4.2 that there is no significant difference in cell viability between the control hDPSCs and the hDPSCs in contact with 70S and 70STi at any

timepoint. This result indicates that the presence of Ti in solution at early timepoints does not have a negative effect on cell viability.

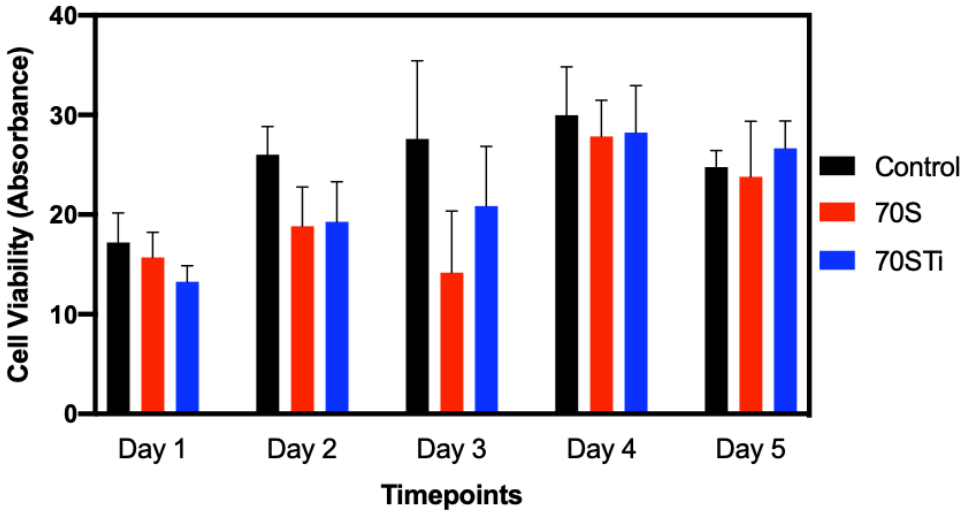

Figure 4.2: Cell proliferation results for hDPSCs grown on tissue culture polystyrene as a control (black) or in the presence of 70S (red) and 70STi (blue) as measured for up to 5 days by an Alamar Blue assay

We also saw in Chapter 3 that both glasses release Si and Ca during the mineralization process as ionic dissolution products. Previous works have demonstrated that ionic release of products from bioactive glass does not have an adverse effect on cell viability or an inhibitory effect on cell metabolic activity [114]. As we see in our study, previous works show that cells in contact with bioactive glass or bioactive glass ionic dissolution products will proliferate at a comparable rate to control cells, grown without exposure to bioactive glass [54, 114].

This is in keeping with previous works that have examined the inclusion of Ti in synthetic HA with no negative effect on cell viability [14, 80]. The results relative to a higher concentration of glass

per well (2mg/well), shown in Figure S2.1, show no change in viability. Thus, 70STi is non-toxic regardless of concentration.

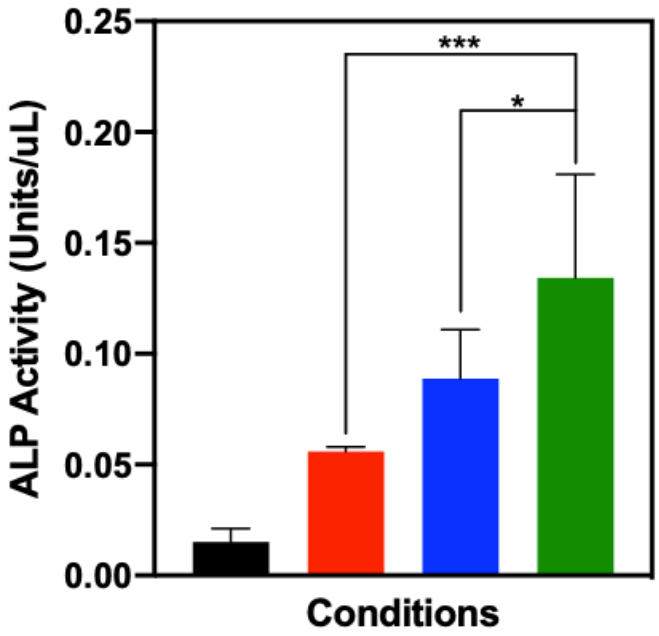

Figure 4.3: ALP activity of hDPSCs cultured in the presence of 70S and 70STi: control hDPSCs in non-osteogenic media (black), control hDPSCs in osteogenic media (red), hDPSCs in contact with 70S in osteogenic media (blue), hDPSCs in contact with 70STi in osteogenic media (green)

Alkaline phosphatase activity (ALP) is an early cell marker for osteoblasts, as it initiates the process of osteoid calcification [115]. We look for increasing ALP activity in cell assays to mark the transition toward osteoblastic differentiation [116]. **Error! Reference source not found.**4.3 shows the results for ALP activity in hDPSCs, cultured in the presence of 70S and 70STi. hDPSCS grown in non-osteogenic media (black), give low levels of ALP activity. With the addition of osteogenic factors to the media (red), hDPSCs show significantly more ALP activity ($p<0.03$). hDPSCs in osteogenic media in the presence of 70S (blue) and 70STi (green) show higher levels of ALP activity. There is a significant ($p<0.002$) increase in ALP activity for hDPSCs in contact with 70STi in osteogenic media compared to control cells in osteogenic media. There is also a

significant ($p<0.032$) difference between hDPSCs in contact with 70S and 70STi, indicating that the presence of Ti on the material surface is the key factor in the increased ALP activity.

An increase in ALP activity in the presence of bioactive glass is well established, as the ionic dissolution products released during HA formation promote osteogenic differentiation [67, 117, 118]. In addition, previous works examining the inclusion of Ti in synthetic HA show that the presence of Ti on the material surface induces significantly more osteogenic differentiation compared to unmodified HA [14, 82]. Our results demonstrate that this increase in osteogenic differentiation ability holds true for 70STi as it undergoes the transformation to a Ti-substituted HA layer.

4.4 Conclusions

In this chapter, we examine our final research objective: how Ti inclusion in bioactive glass effects cell viability and osteogenic differentiation. Our results show that the 70STi is non-toxic to cells and in fact significantly increases osteogenic differentiation when compared to 70S. We replicate trends from literature indicating that Ti is the main contributing factor in the increased osteogenic ability of this material. Based on these experiments, 70STi has applications that range beyond dentistry into the broader field of bone tissue engineering. It could act as an active repair agent for hard tissue, as it releases ionic dissolution products that promote cellular and genetic responses favorable to mineralization while maintaining a surface that promotes osteoblast adhesion and differentiation.

Future work will investigate 70STi for a broader range of properties including antibacterial, and response in an animal model. We will also put compositions with lower and higher Ti additions in contact with cells. One of these compositions may promote an increased osteogenic effect.

Chapter 5: Concluding Remarks and Perspectives

5.1 Conclusions

At the beginning of this thesis, we laid out three research objectives that covered investigating 70STi from synthesis to cellular studies. Through our experiments in Chapter 4 we answered our first two objectives. We synthesised a Ti-containing bioactive glass through the sol-gel method with high specific surface area and porosity that is comparable to other sol-gel glasses of similar composition. The glass remains fully amorphous despite addition of Ti. Through XPS and EDS, we see that Ti is homogenously distributed throughout the glass.

70STi is reactive in SBF, forming a HA layer on the surface of the glass. Previous works did not study if and how Ti inclusion in bioactive glasses would be incorporated in the eventual HA layer formed on the surface of the glasses. In our work, we show that Ti is retained within the glass and eventual HA layer during mineralization, rather than released to solution. This differentiates 70STi from previous glass compositions that include Ti, where the goal was to release Ti to the local environment.

This material is a good candidate for enamel remineralization. We see in literature that the presence of Ti in native enamel, delivered through candy/gum ingestion, is correlated with increased tooth hardness and brightness. Our glass works as an active repair agent for HA in addition to providing a controllable Ti delivery vehicle. This is an improvement on current remineralization technology.

In Chapter 5, we show that 70STi is non-toxic to cells, illustrating that this material is biocompatible in addition to being bioactive. While enamel is acellular, biocompatibility is important as any remineralization treatment would likely make some contact with the local cellular environment. This opens the material up to applications beyond dentistry. We demonstrate that the inclusion of Ti in 70STi results in a significantly improved osteogenic response compared to 70S, making it an interesting material for bone tissue engineering. This requires further work to determine where 70STi would be the best candidate. However, from

previous work involving Ti-containing HA, we hypothesize that 70STi may possess improved mechanical properties compared to undoped bioactive glass. One drawback of the use of current bioactive glasses in bone tissue engineering is their inherent brittleness. This limits their use in load bearing applications. 70STi may be an improvement on current compositions for this application. This hypothesis will be investigated in future experiments.

5.2 Future Perspectives

The three research objects give us a good starting place for understanding 70STi from structure, to mineralization behaviour to cellular response. We now want to go beyond this basic knowledge to determine specific applications for 70STi. We propose several experiments to do this. These are broken down into experiments that relate to enamel remineralization and to the broader field of bone tissue engineering:

(i) ***Enamel remineralization:*** We draw inspiration from previous enamel remineralization studies using bioactive glass. These studies use a simple in vitro model. Donor teeth are demineralized in an acid solution, to expose dental tubules [51]. Bioactive glass powder is then brushed onto the teeth twice a day and stored in a simulated saliva solution, allowing the bioactive glass to react and remineralize the tooth. We propose using this model with 70STi to study its ability to remineralize enamel. As in Chapter 4, we would analyze the formation of the Ti-containing HA layer through FTIR, XRD, SEM, EDS, and XPS. Once mineralized, the properties of the Ti HA layer would be analyzed with respect to clinical concerns such as increased tooth hardness and brightness. This would be conducted through microhardness testing and shade measurements respectively.

Through these experiments, we will see if 70STi acts as an active repair agent while delivering Ti to improve clinically desirable properties of the enamel layer. If this is the case, we believe that this glass has great potential for commercialization. Large companies such as Sensodyne already recognize the benefits of bioactive glass in dentistry, opening the door for new materials like 70STi.

(ii) ***Bone tissue engineering:*** This thesis only provides very basic experiments related to bone tissue engineering. However, the osteogenic results from 70STi make it an interesting material moving forward. We require more cell experiments to look at both the osteogenic (bone forming) and angiogenic (blood vessel forming) cell response. Incorporation of 70STi in a scaffold would allow us to test an in vivo response in a rat or mouse model. Scaffolds will also allow us to examine if and how 70STi may have impact on mechanical properties. We also suggest conducting antibacterial experiments to see if Ti inclusion improves those properties compared to both undoped bioactive glasses and doped bioactive glasses that have previously demonstrated an antibacterial response.

References:

[1] C. Robinson, J. Kirkham, R. Shore, Dental Enamel: Formation to Destruction, CRC Press, Boca Raton, Florida 1995.
[2] E. Ghadimi, H. Eimar, B. Marelli, S.N. Nazhat, M. Asgharian, H. Vali, F. Tamimi, Trace elements can influence the physical properties of tooth enamel, SpringerPlus 2(1) (2013) 499.
[3] T. Vargas-Koudriavtsev, R. Durán-Sedó, Ó.-A. Herrera-Sancho, Titanium dioxide in dental enamel as a trace element and its variation with bleaching, J Clin Exp Dent 10(6) (2018) e537-e541.
[4] X. Li, J. Wang, A. Joiner, J. Chang, The remineralization of enamel: a review of the literature, Journal of Dentistry 42(1) (2014) 12-20.
[5] M. Shahmoradi, L.E. Bertanssoni, H.M. Elfallah, M.V. Swain, Advances in Calcium Phosphate Biomaterials Springer Berlin Heidelberg 2014.
[6] L. Hench, R. Splinter, W. Allen, T. Greenlee, Bonding mechanisms at the interface of ceramic prosthetic materials Journal of Biomedical Materials Research 5 (1971) 117-141.
[7] J.R. Jones, Review of bioactive glass: From Hench to hybrids, Acta Biomaterialia 9(1) (2013) 4457-4486.
[8] F. Baino, S. Hamzehlou, S. Kargozar, Bioactive Glasses: Where Are We and Where Are We Going?, Journal of Functional Biomaterials 9(25) (2018).
[9] F. Baino, E. Fiume, M. Miola, E. Verné, Bioactive sol-gel glasses: Processing, properties, and applications, International Journal of Applied Ceramic Technology 15(4) (2018) 841-860.
[10] S. Nandi, A. Mahato, B. Kundu, P. Mukherjee, Doped Bioactive Glass Materials in Bone Regeneration, 2016.
[11] L.L. Hench, The story of Bioglass®, Journal of Materials Science: Materials in Medicine 17(11) (2006) 967-978.
[12] Y. Li, Fabrication and Applications of Metal-Ion-Doped Hydroxyapatite Nanoparticles, Juniper Online Journal Material Science 1 (2017).
[13] A. Hu, M. Li, C. Chang, D. Mao, Preparation and characterization of a titanium-substituted hydroxyapatite photocatalyst, Journal of Molecular Catalysis A: Chemical 267(1) (2007) 79-85.
[14] J. Huang, S. Best, W. Bonfield, T. Buckland, Development and characterization of titanium-containing hydroxyapatite for medical applications, Acta Biomaterialia 6 (2010) 241-249.
[15] Y. Ozbek, F. Bastan, N. Canikoğlu, U. Ozsarac, The experimental study of titanium-ions into hydroxyapatite by chemical precipitation, Journal of Thermal Analysis and Calorimetry 125 (2016) 651-658.
[16] M. Sato, E.B. Slamovich, T.J. Webster, Enhanced osteoblast adhesion on hydrothermally treated hydroxyapatite/titania/poly(lactide-co-glycolide) sol–gel titanium coatings, Biomaterials 26(12) (2005) 1349-1357.
[17] C.D. Association, The State of Oral Health in Canada in: C.D. Association (Ed.) 2017.
[18] K. Lin, J. Chang, 1 - Structure and properties of hydroxyapatite for biomedical applications, in: M. Mucalo (Ed.), Hydroxyapatite (Hap) for Biomedical Applications, Woodhead Publishing2015, pp. 3-19.
[19] S. Rujitanapanich, P. Kumpapan, P. Wanjanoi, Synthesis of Hydroxyapatite from Oyster Shell via Precipitation, Energy Procedia 56 (2014) 112–117.

[20] H. Aguiar, J. Serra, P. González, B. León, Structural study of sol–gel silicate glasses by IR and Raman spectroscopies, Journal of Non-Crystalline Solids 355(8) (2009) 475-480.
[21] T. Tite, A.-C. Popa, L.M. Balescu, I.M. Bogdan, I. Pasuk, J.M.F. Ferreira, G.E. Stan, Cationic Substitutions in Hydroxyapatite: Current Status of the Derived Biofunctional Effects and Their In Vitro Interrogation Methods, Materials (Basel) 11(11) (2018) 2081.
[22] J.P. Simmer, J.C.-C. Hu, Dental Enamel Formation and Its Impact on Clinical Dentistry Journal of Dental Education 65(9) (2001) 896-905.
[23] R. Söremark, K. Samahl, Gamma-ray spectrometric analysis of elements in normal human enamel, Archive of Oral Biology 6 (1961) 275-283.
[24] R.A. Terpstra, F.C.M. Driessens, Magnesium in Tooth Enamel and Synthetic Apatites Calcified Tissue International 39 (1986) 348-354.
[25] T. Aoba, The effect of fluoride on apatite structure and growth, Crit Rev Oral Biol Med 8(2) (1997) 136-53.
[26] E.A.A. Neel, A. Aljabo, A. Strange, S. Ibrahim, M. Coathup, A.M. Young, L. Bozec, V. Mudera, Demineralization-remineralization dynamics in teeth and bone, International Journal of Nanomedicine 11 (2016) 4743-4763.
[27] Sangi, Consumer Benefits, 2011. http://www.sangi-co.com/en/technology/consumer_benefits/index.html.
[28] S. Baliga, S. Muglikar, R. Kale, Salivary pH: A diagnostic biomarker, J Indian Soc Periodontal 17(4) (2013) 461-465.
[29] J.D.B. Featherstone, Dental caries: a dynamic disease process, Australian Dental Journal 53 (2008) 286-291.
[30] E. Mizrahi, Enamel demineralization following orthodontic treatment American Journal of Orthodontics and Dentofacial Orthopedics 82(2) (1982) 62-67.
[31] Y. Ren, M.A. Jongsma, L. Mei, H.C.v.d. Mei, H.J. Busscher, Orthodontic treatment with fixed applications and biofilm formation - a potential public health threat?, Clinical Oral Investigations 18(7) (2014) 1711-8.
[32] Y.-Q. Wu, J.A. Arsecularatne, M. Hoffman, Attrition-corrosion of human dental enamel: A review, Biosurface and Biotribology 3 (2017) 196-210.
[33] S.H. Ashoor, M.J. Knox, Determination of organic acids in foods by high-performance liquid chromatography Journal of Chromatography 299 (1984) 288-292.
[34] A. Lussi, T. Jaeggi, Erosion-diagnosis and risk factors, Clinical Oral Investigations 12 (2008) 5-13.
[35] P.E. Petersen, The World Oral Health Report 2003: Continuous improvement of oral health in the 21st century - the approach to the WHO Global Oral Health Programme, World Health Organization, Geneva 2003.
[36] F.W.D. Federation, Oral Health Worldwide. A report by FDI World Dental Association, FDI World Dental Federation, Switzerland, 2014.
[37] OECD, Health at a Glance 2013: OECD Indicators, OECD Publishing, Paris, 2013.
[38] M.A.R. Buzalaf, A.R. Hannas, M.T. Kato, Saliva and dental erosion, Journal of Applied Oral Science 20(5) (2012) 493-502.
[39] F. Lippert, D.M. Parker, K.D. Jandt, In vitro demineralization/remineralization cycles at human tooth enamal surfaces investigated by AFM and nanoindentation, Colloid and Interface Science 280 (2014) 442-448.

[40] Y. Tanizawa, H. Tsuchikane, K. Sawamura, Reaction Characteristics of Hydroxyapatite with F- and PO3F2- ions, J Chem Soc Faraday Trans 87(14) (1991) 2235-2240.
[41] G.S. Ingram, P.F. Nash, A Mechanism for the Anticaries Action of Fluoride Caries Research 14 (1980) 298-303.
[42] J.A. Cury, L.M.A. Tenuta, Enamel remineralization: controlling the caries diseas or treating early caries lesions?, Brazilian Oral Research 23 (2009) 23-30.
[43] E.I.F. Pearce, D.G.A. Nelson, In vivo comparison of caries inhibition by a plaque mineral enriching mouthrinse and fluoride dentifrice, Caries Research 22 (1988) 362-370.
[44] M. Lelli, A. Putignano, M. Marchetti, I. Foltran, F. Mangani, M. Procaccini, N. Roveri, G. Orsini, Remineralization and repair of enamel surface by biomimetic Zn-carbonate hydroxyapatite containing toothpaste:a comparative in vivo study, Fronteirs in Physiology 5 (2014).
[45] P. Tschoppe, D.L. Zandim, P. Martus, A.M. Kielbassa, Enamel and dentine remineralization by nano-hydroxyapatite toothpastes, Journal of Dentistry 39 (2011) 430-437.
[46] C. Fowler, R. Wilson, G.D. Rees, In vitro microhardness studies on a new anti-erosion desensitizing toothpaste, Journal of Clinical Dentistry 17 (2006) 100-105.
[47] J.P. Pessan, S.M.B. Silva, J. Lauris, F.C. Sampaio, G.M. Whitford, M.A.R. Buzalaf, Fluoride uptake by plaque from water and from dentifrice, Journal of Dental Research 87 (2008) 461-465.
[48] K. Hornby, M. Evans, M. Long, A. Joiner, M. Laucello, A. Salvaderi, Enamel benefits of a new hydroxyapatite containing fluoride toothpaste, International Dental Journal 59 (2009) 325-331.
[49] D. Shi, Biomaterials and Tissue Engineering, Springer, New York 2004.
[50] V. Miguez-Pacheco, D. Greenspan, L. Hench, A. Boccaccini, Bioactive glasses in soft tissue repair American Ceramic Society Bulletin 94(6) (2006) 27-31.
[51] Z. Abbasi, M. Bahrololoom, M. Shariat, R. Bagheri, Bioactive glasses in dentistry: a review, Journal of Dental Biomaterials 2(1) (2015).
[52] S.M. Rabiee, N. Nazparvar, M. Azizian, D. Vashaee, L. Tayebi, Effect of ion substitution on properties of bioactive glasses: a review, Ceramics International 41(6) (2015) 7241-7251.
[53] S. Biomedical, BioSphere Technology - Bioactive Glass Properties, 2017. https://www.synergybiomedical.com/bioactive-glass-properties.html.
[54] A. Hoppe, N.S. Güldal, A.R. Boccaccini, A review of the biological response to ionic dissolution products from bioactive glasses and glass-ceramics, Biomaterials 32(11) (2011) 2757-2774.
[55] Q. Fu, E. Saiz, M.N. Rahaman, A.P. Tomsia, Bioactive glass scaffolds for bone tissue engineering: state of the art and future perspectives, Materials science & engineering. C, Materials for biological applications 31(7) (2011) 1245-1256.
[56] H. Palza, B. Escobar, J. Bejarano, D. Bravo, M. Diaz-Dosque, J. Perez, Designing antimicrobial bioactive glass materials with embedded metal ions synthesized by the sol–gel method, Materials Science and Engineering: C 33(7) (2013) 3795-3801.
[57] X. Liu, M.N. Rahaman, D.E. Day, In Vitro Degradation and Conversion of Melt-Derived Microfibrous Borate (13-93B3) Bioactive Glass Doped with Metal Ions, Journal of the American Ceramic Society 97(11) (2014) 3501-3509.
[58] B. Tai, Z. Bian, H. Jiang, D. Greenspan, J. Zhong, A. Clark, Anti-gingivitis effect of a dentifrice containing bioactive glass (NovaMin®) particulate, Journal of Clinical Periodontology 32(2) (2006) 89-91.

[59] J. Earl, R. Leary, K. Muller, R. Langford, D. Greenspan, Physical and chemical characterization of dentin surface following treatment with NovaMin technology., Journal of Clinical Dentistry 22(3) (2011) 62-67.
[60] Z. Wang, T. Jiang, S. Sauro, The dentine mineralization activity of a desensitizing bioactive glass-containing toothpaste: an in vitro review, Australian Dental Journal 56 (2011) 372-381.
[61] A. Mehta, V. Kumari, R. Jose, Remineralization potential of bioactive glass and casein phosphopeptide-amorphous calcium phosphate on initial carious lesion: an in vitro pH-cycling study, J Conserv Dent 17 (2014) 3-7.
[62] GSK, Novamin - the accidental curist, 2014. https://www.gsk.com/en-gb/behind-the-science/patients-consumers/novamin-the-accidental-curist/.
[63] C. Brinker, G. Scherer, Sol-Gel Science: The Physics and Chemistry of Sol-gel Processing Academic Press2013.
[64] S.P. Mukherjee, Sol-gel processes in glass science and technology, Journal of Non-Crystalline Solids 42(1) (1980) 477-488.
[65] J. Zhong, D.C. Greenspan, Processing and Properties of sol-gel bioactive glasses Journal of Biomedical Materials Research 53(6) (2000) 694-701.
[66] T. Albrektsson, C. Johansson, Osteoinduction, osteoconduction and osseointegration, Eur Spine J 10 Suppl 2 (2001) S96-101.
[67] J.E. Gough, J.R. Jones, L.L. Hench, Nodule formation and mineralisation of human primary osteoblasts cultured on a porous bioactive glass scaffold, Biomaterials 25(11) (2004) 2039-2046.
[68] I.D. Xynos, A.J. Edgar, L.D.K. Buttery, L.L. Hench, J.M. Polak, Gene-expression profiling of human osteoblasts following treatment with the ionic products of Bioglass® 45S5 dissolution, Journal of Biomedical Materials Research 55(2) (2001) 151-157.
[69] E. Fiume, J. Barberi, E. Verné, F. Baino, Bioactive Glasses: From Parent 45S5 Composition to Scaffold-Assisted Tissue-Healing Therapies, Journal of functional biomaterials 9(1) (2018) 24.
[70] S. Maeno, Y. Niki, H. Matsumoto, H. Morioka, T. Yatabe, A. Funayama, Y. Toyama, T. Taguchi, J. Tanaka, The effect of calcium ion concentration on osteoblast viability, proliferation and differentiation in monolayer and 3D culture, Biomaterials 26(23) (2005) 4847-4855.
[71] A. Bigi, The role of magnesium on the structure of biological apatites Calcified Tissue International 50(5) (1992) 69-78.
[72] F. Ren, Synthesis, characterization, and ab inito simulation of magnesium substituted hydroxyapatite Acta Biomaterialia 6(7) (2010) 2787-2796.
[73] Y. Wang, H. Chang, Y. Chiang, C. Lin, C. Lin, Strontium ion can significantly decrease enamel demineralization and prevent the enamel surface hardness loss in acidic environment, Journal of the Formosan Medical Association (2018).
[74] M. Frasnelli, F. Cristofaro, V.M. Sglavo, S. Dirè, E. Callone, R. Ceccato, G. Bruni, A.I. Cornaglia, L. Visai, Synthesis and characterization of strontium-substituted hydroxyapatite nanoparticles for bone regeneration, Materials Science and Engineering: C 71 (2017) 653-662.
[75] N. Zahra, M. Fayyaz, W. Iqbal, M. Irfan, S. Alam, A process for the development of strontium hydroxyapatite, IOP Conference Series: Materials Science and Engineering 60 (2014) 012056.
[76] J. Huang, S.M. Best, W. Bonfield, T. Buckland, Development and characterization of titanium-containing hydroxyapatite for medical applications, Acta Biomaterialia 6(1) (2010) 241-249.

[77] A. Weir, P. Westerhoff, L. Fabricius, K. Hristovski, N. von Goetz, Titanium Dioxide Nanoparticles in Food and Personal Care Products, Environmental Science & Technology 46(4) (2012) 2242-2250.
[78] Z.B.H.A.R. Zeeshan Qamar, Hooi Pin Chew, Tayyaba Fatima, Influence of trace elements on dental enamel properties: A review, J Pak Med Assoc 67(1) (2017) 116-120.
[79] C. Ergun, Effect of Ti ion substitution on the structure of hydroxylapatite, Journal of the European Ceramic Society 28 (2008) 2137-2149.
[80] I.-C. Brie, O. Soritau, N. Dirzu, C. Berce, A. Vulpoi, C. Popa, M. Todea, S. Simon, M. Perde-Schrepler, P. Virag, O. Barbos, G. Chereches, P. Berce, V. Cernea, Comparative in vitro study regarding the biocompatibility of titanium-base composites infiltrated with hydroxyapatite or silicatitanate, Journal of Biological Engineering 8(1) (2014) 14.
[81] C.C. Ribeiro, I. Gibson, M.A. Barbosa, The uptake of titanium ions by hydroxyapatite particles—structural changes and possible mechanisms, Biomaterials 27(9) (2006) 1749-1761.
[82] C. Ergun, H. Liu, J.W. Halloran, T.J. Webster, Increased osteoblast adhesion on nanograined hydroxyapatite and tricalcium phosphate containing calcium titanate, Journal of Biomedical Materials Research Part A 80A(4) (2007) 990-997.
[83] P.A. Ramires, A. Romito, F. Cosentino, E. Milella, The influence of titania/hydroxyapatite composite coatings on in vitro osteoblasts behaviour, Biomaterials 22(12) (2001) 1467-1474.
[84] I. Kashif, A.A. Soliman, H. Farouk, A.M. Sanad, Effect of titanium addition on crystallization kinetics of lithium borosilicate glass, Journal of Alloys and Compounds 475(1) (2009) 712-717.
[85] S. Ni, R. Du, S. Ni, The Influence of Na and Ti on the In Vitro Degradation and Bioactivity in 58S Sol-Gel Bioactive Glass, Advances in Materials Science and Engineering 2012 (2012) 7.
[86] O. Rodriguez, W. Stone, E.H. Schemitsch, P. Zalzal, S. Waldman, M. Papini, M.R. Towler, Titanium addition influences antibacterial activity of bioactive glass coatings on metallic implants, Heliyon 3(10) (2017) e00420-e00420.
[87] A.W. Wren, F.R. Laffir, A. Kidari, M.R. Towler, The structural role of titanium in Ca–Sr–Zn–Si/Ti glasses for medical applications, Journal of Non-Crystalline Solids 357(3) (2011) 1021-1026.
[88] D.S. Brauer, N. Karpukhina, R.V. Law, R.G. Hill, Effect of TiO2 addition on structure, solubility and crystallisation of phosphate invert glasses for biomedical applications, Journal of Non-Crystalline Solids 356(44) (2010) 2626-2633.
[89] N. Mohammed, R. Lynch, P. Anderson, Inhibitory effects of Zinc Ions on Enamel Demineralization Kinetics in vitro, Caries Research 49(6) (2015) 600-605.
[90] T.H. Kokubo T., Simulated Body Fluid (SBF) as a Standard Tool to Test the Bioactivity of Implants, Handbook of Biomineralization2007, pp. 97-109.
[91] J. Román, S. Padilla, M. Vallet-Regí, Sol−Gel Glasses as Precursors of Bioactive Glass Ceramics, Chemistry of Materials 15(3) (2003) 798-806.
[92] L.M. Mukundan, R. Nirmal, D. Vaikkath, P.D. Nair, A new synthesis route to high surface area sol gel bioactive glass through alcohol washing: a preliminary study, Biomatter 3(2) (2013) e24288.
[93] A. Balamurugan, G. Sockalingum, J. Michel, J. Fauré, V. Banchet, L. Wortham, S. Bouthors, D. Laurent-Maquin, G. Balossier, Synthesis and characterisation of sol gel derived bioactive glass for biomedical applications, Materials Letters 60(29) (2006) 3752-3757.

[94] A. Lucas-Girot, F.Z. Mezahi, M. Mami, H. Oudadesse, A. Harabi, M. Le Floch, Sol–gel synthesis of a new composition of bioactive glass in the quaternary system SiO2–CaO–Na2O–P2O5: Comparison with melting method, Journal of Non-Crystalline Solids 357(18) (2011) 3322-3327.
[95] L. Radev, K. Hristova, V. Jordanov, M. Fernandes, I. Margarida M. Salvado, In vitro bioactivity of 70 wt.% SiO2 — 30 wt.% CaO sol-gel glass, doped with 1, 3 and 5 wt.% NbF5, 2011.
[96] J. Serra, P. González, S. Liste, C. Serra, S. Chiussi, B. León, M. Pérez-Amor, H.O. Ylänen, M. Hupa, FTIR and XPS studies of bioactive silica based glasses, Journal of Non-Crystalline Solids 332(1) (2003) 20-27.
[97] C. Ergun, Effect of Ti ion substitution on the structure of hydroxylapatite, Journal of the European Ceramic Society 28(11) (2008) 2137-2149.
[98] A. Ramos, M. Gandais, Earliest stages of crystal growth in a silicate glass containing titanium and zirconium as nucleating elements — HRTEM and XAS study, Journal of Crystal Growth 100(3) (1990) 471-480.
[99] B.E. Warren, X-ray Diffraction Study of the Structure of Glass, Chemical Reviews 26(2) (1940) 237-255.
[100] A.L.B. Maçon, T. B Kim, E. Valliant, K. Goetschius, R. Brow, D. E Day, A. Hoppe, A. Boccaccini, I. Yong Kim, C. Ohtsuki, T. Kokubo, A. Osaka, M. Vallet-Regí, D. Arcos, L. Fraile, A. Salinas, A. V Teixeira, Y. Vueva, R. Almeida, J. Jones, A unified in vitro evaluation for apatite-forming ability of bioactive glasses and their variants, Journal of materials science. Materials in medicine 26 (2015) 5403.
[101] A. Lukowiak, J. Lao, J. Lacroix, J.-M. Nedelec, Bioactive glass nanoparticles obtained through sol–gel chemistry, Chemical Communications 49(59) (2013) 6620-6622.
[102] W.C. Lepry, S. Naseri, S.N. Nazhat, Effect of processing parameters on textural and bioactive properties of sol–gel-derived borate glasses, Journal of Materials Science 52(15) (2017) 8973-8985.
[103] S.M. Londoño-Restrepo, L.F. Zubieta-Otero, R. Jeronimo-Cruz, M.A. Mondragon, M.E. Rodriguez-García, Effect of the Crystal Size of Biogenic Hydroxyapatites on IR and Raman Spectra, bioRxiv (2018) 465146.
[104] L. Berzina-Cimdina, N. Borodajenko, Research of Calcium Phosphates Using Fourier Transform Infrared Spectroscopy, 2012.
[105] P. Sepulveda, J. Jones, L. Hench, Characterization of melt-derived 45S5 and sol-gel-derived 58S bioactive glasses, Journal of biomedical materials research 58 (2001) 734-40.
[106] R. Li, A.E. Clark, L.L. Hench, An investigation of bioactive glass powders by sol-gel processing, Journal of Applied Biomaterials 2(4) (1991) 231-239.
[107] M. Cerruti, C.L. Bianchi, F. Bonino, A. Damin, A. Perardi, C. Morterra, Surface Modifications of Bioglass Immersed in TRIS-Buffered Solution. A Multitechnical Spectroscopic Study, The Journal of Physical Chemistry B 109(30) (2005) 14496-14505.
[108] M. Cerruti, C. Morterra, Carbonate Formation on Bioactive Glasses, Langmuir : the ACS journal of surfaces and colloids 20 (2004) 6382-8.
[109] A. Bari, N. Bloise, S. Fiorilli, G. Novajra, M. Vallet-Regí, G. Bruni, A. Torres-Pardo, J.M. González-Calbet, L. Visai, C. Vitale-Brovarone, Copper-containing mesoporous bioactive glass nanoparticles as multifunctional agent for bone regeneration, Acta Biomaterialia 55 (2017) 493-504.

[110] E. Mancuso, O.A. Bretcanu, M. Marshall, M.A. Birch, A.W. McCaskie, K.W. Dalgarno, Novel bioglasses for bone tissue repair and regeneration: Effect of glass design on sintering ability, ion release and biocompatibility, Mater Des 129 (2017) 239-248.
[111] M. Bakkar, Y. Liu, D. Fang, C. Stegen, X. Su, M. Ramamoorthi, L.-C. Lin, T. Kawasaki, N. Makhoul, H. Pham, Y. Sumita, S.D. Tran, A Simplified and Systematic Method to Isolate, Culture, and Characterize Multiple Types of Human Dental Stem Cells from a Single Tooth, in: P. Di Nardo, S. Dhingra, D.K. Singla (Eds.), Adult Stem Cells: Methods and Protocols, Springer New York, New York, NY, 2017, pp. 191-207.
[112] S. Gronthos, J. Brahim, W. Li, L.W. Fisher, N. Cherman, A. Boyde, P. DenBesten, P.G. Robey, S. Shi, Stem cell properties of human dental pulp stem cells, J Dent Res 81(8) (2002) 531-5.
[113] L.L. Hench, I. Thompson, Twenty-first century challenges for biomaterials, J R Soc Interface 7 Suppl 4(Suppl 4) (2010) S379-S391.
[114] S. Gholami, S. Labbaf, A. Baharlou Houreh, H.-K. Ting, J. Jones, M.-H. Esfahani, Long term effects of bioactive glass particulates on dental pulp stem cells in vitro, Biomedical Glasses 3 (2017).
[115] A. Rutkovskiy, K.-O. Stensløkken, I.J. Vaage, Osteoblast Differentiation at a Glance, Med Sci Monit Basic Res 22 (2016) 95-106.
[116] E.E. Golub, K. Boesze-Battaglia, The role of alkaline phosphatase in mineralization, Current Opinion in Orthopaedics 18(5) (2007) 444-448.
[117] M. Ojansivu, S. Vanhatupa, L. Björkvik, H. Häkkänen, M. Kellomäki, R. Autio, J.A. Ihalainen, L. Hupa, S. Miettinen, Bioactive glass ions as strong enhancers of osteogenic differentiation in human adipose stem cells, Acta Biomaterialia 21 (2015) 190-203.
[118] M. Bosetti, M. Cannas, The effect of bioactive glasses on bone marrow stromal cells differentiation, Biomaterials 26(18) (2005) 3873-3879.
[119] N. Gupta, D. Santhiya, 3 - Mesoporous bioactive glass and its applications, in: H. Ylänen (Ed.), Bioactive Glasses (Second Edition), Woodhead Publishing2018, pp. 63-85.

Supporting Information

EDS of 70S AM

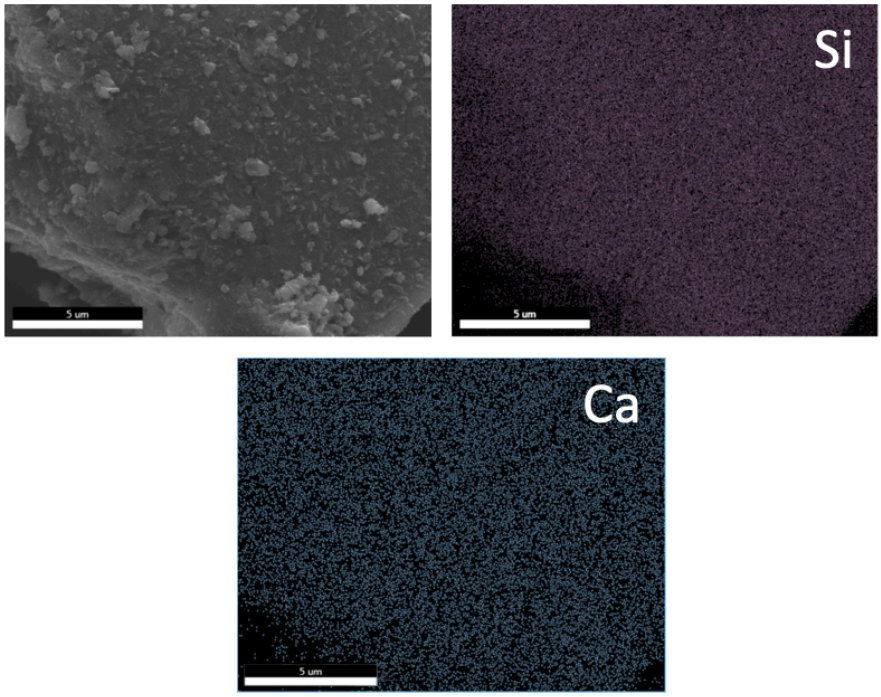

Figure S1.1: EDS elemental mapping of 70S as made (scale bar = 5μm)

The elemental mapping shows the distribution of Si and calcium throughout the as made control glass. Si is the most prominent element and is densely but evenly indicated across the entirety of the image. Calcium is also observed and is evenly distributed across the sample.

Powder distribution

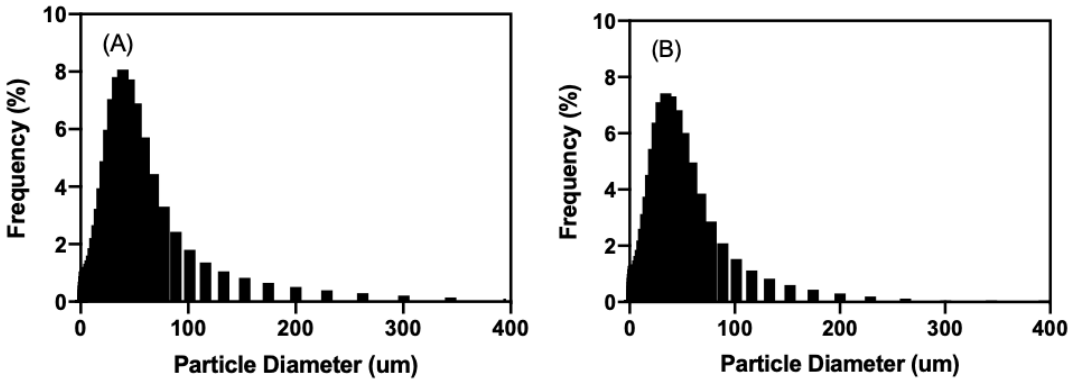

Figure S1.2: Powder Size Distribution (A) 70S, (B) 70STi

The powder size distribution is an important factor to consider to be able to directly compare the mineralization behaviour of multiple powdered glass samples. In this study, the powders were manually ground down and size excluded through manual sieving to a size class of 25-45μm. As seen in Figure S1.2 the two glasses have a similar, unimodal distribution with average particle diameter of ~36μm. For both samples, there is a trailing tail end towards higher particle diameters (>100μm). However, the frequency for these size classes is very low

Isotherms

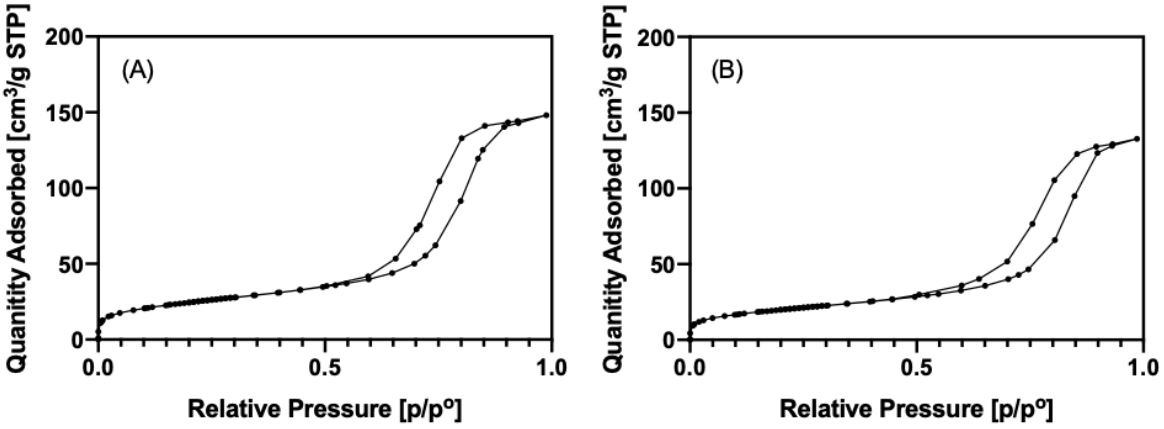

Figure S1.3: Linear isotherm plot for 70S (A) and 70STi (B) during surface area measurements through BET

70STi shows lower surface area through lower adsorption quantity compared to 70S. Both samples exhibit Type IV isotherm behaviour with a hysteresis loop, indicating the presence of mesopores [119].

Isotherms of mineralized 70S

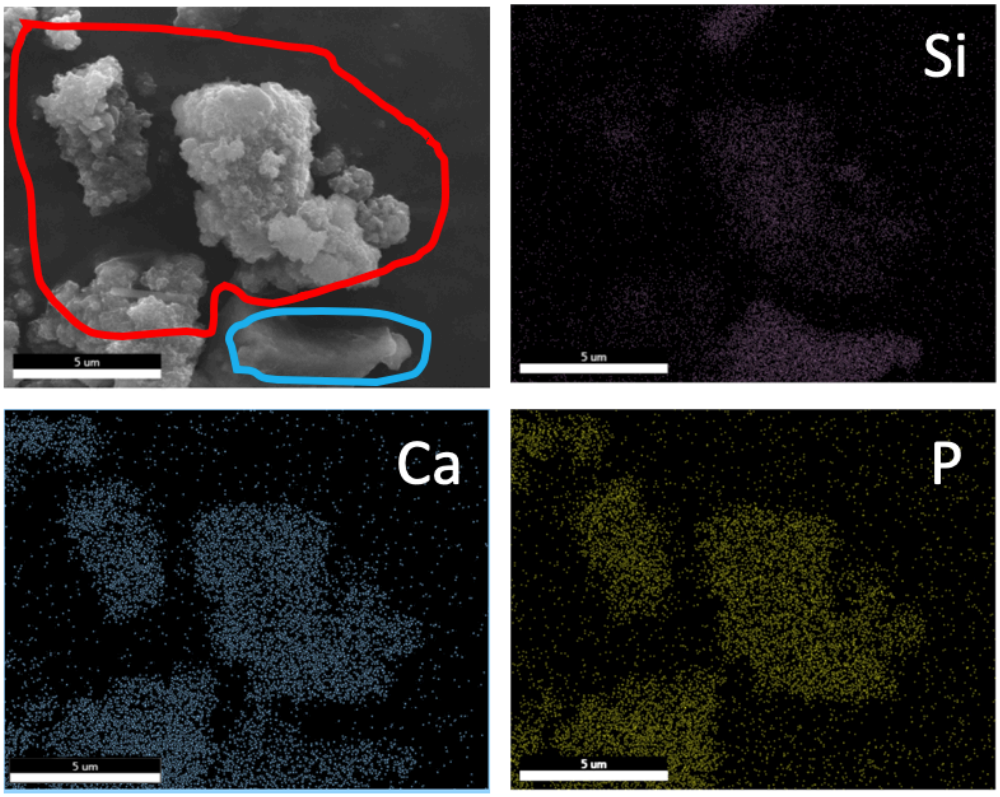

Figure S1.4: Elemental mapping of 70S after 7 days of immersion in SBF (scale bar = 5μm)

After immersion in SBF for 7 days, the control glass has a distinct layer of hydroxyapatite formed on the surface. In area 1 (outlined in red), mineralized glass shows morphology characteristic of hydroxyapatite formation. In area 2 (outlined in blue), a glass particle that remains in the early stages of mineralization. Si signal is less prominent in area 1, as it is being covered by the calcium phosphorus layer. However, the Si shows more strongly for area 2, the glass that is not fully mineralized, in a pattern that is consistent with the as-made glass.

P is strongly present in area 1. The element is not present in the as-made glass composition so does not appear as strongly in area 2. However, small amounts of P are seen in that area, indicating that the glass is in the process of hydroxyapatite formation. Calcium is evenly distributed across the material as it is for the as made glass. The signal is stronger for areas that are mineralized, calcium has migrated to the surface of the material as well as being precipitated on to the surface from the SBF solution.

Cell Response

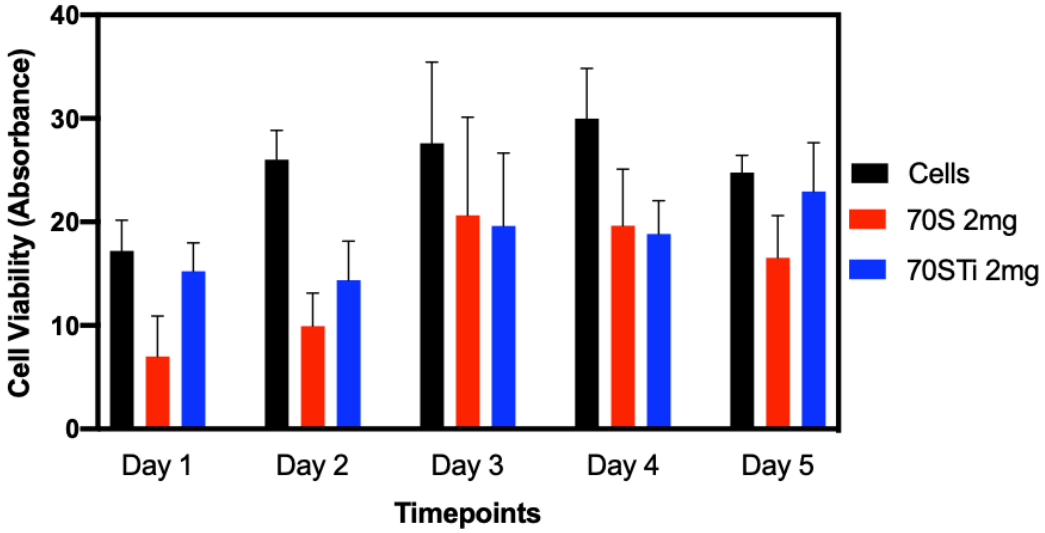

Figure S2.1: Human DPSC cell proliferation in response to the presence of 70S (2mg/well) and 70STi (2mg/well) as measured for up to 5 days by an Alamar Blue assay